Science of the Total Environment 862 (2023) 160747

Contents lists available at ScienceDirect

Science of the Total Environment

journal homepage: www.elsevier.com/locate/scitotenv

Measurement of particulate matter in a heritage building using optical counters: Long-term and spatial analyses

Nuno Baía Saraiva *, Luisa Dias Pereira, Adélio Rodrigues Gaspar, José Joaquim Costa

University of Coimbra, ADAI, Department of Mechanical Engineering, Rua Luís Reis Santos, Pólo II, 3030-788 Coimbra, Portugal

HIGHLIGHTS

- Monitoring, prediction, and analysis of particles using optical counters
- Long-term and spatial analysis of particulate matter in a heritage library
- New classification of indoor pollution from a conservation perspective
- Identification of the main causes of indoor pollution in the heritage building
- Optical counters are useful in the characterization of indoor pollution.

GRAPHICAL ABSTRACT

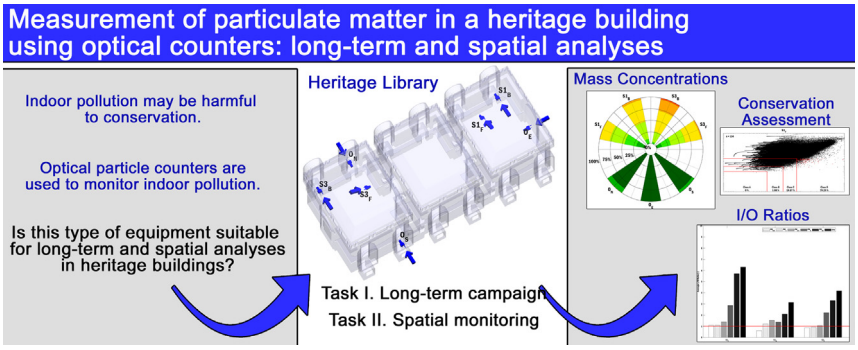

ARTICLE INFO

Editor: Anastasia Paschalidou

Keywords:
Dust
Indoor air quality
Preventive conservation
Historic buildings
Monitoring particles

ABSTRACT

The good conservation of cultural patrimony depends on the quality of the indoor environment where collections and artifacts are kept, being suspended particles one of the key parameters. Among the various methods to study indoor pollution, portable optical counters appear as effective instruments to measure indoor pollution due to their specifications (low visual and acoustic impact). However, it is still one of the least common approaches when assessing the conservation quality in heritage buildings. Therefore, the present study focuses on developing a methodology that uses portable particle counters to monitor particulate matter inside historic buildings and assess indoor conservation quality. Long-term and spatial analyses were conducted using this type of equipment to identify causes of pollution in a case study, the Joanina Library in Coimbra, Portugal. Estimation of night concentrations was carried out as a complementary approach to the monitoring. A new conservation method of classifying indoor pollution was proposed as an alternative to the most common standards. This classification determines four conservation classes (A, B, C, and D) according to particulate matter and the respective percentage of time that measurements are within such classes. As a result, the measurements showed a poor indoor environment quality meeting the requirements of low-level classes, which are those with a greater risk of degradation (Classes C and D). The continuous long-term campaign of four years was decisive for the identification of the main sources and environmental conditions of higher pollution: the exterior pavement, the number of tourists, the use of carpets, and the absence of rain. The spatial results depend on the diameters of the particles and the space's height where the assessment is made. Thus, this type of device and the developed methodology could be used by curators as an effective tool for long-term and spatial assessment in this building typology.

* Corresponding author.
E-mail address: nuno.saraiva@dem.uc.pt (N.B. Saraiva).

http://dx.doi.org/10.1016/j.scitotenv.2022.160747
Received 13 September 2022; Received in revised form 2 December 2022; Accepted 3 December 2022
Available online 7 December 2022

Nomenclature

A	Area of surfaces, m^2
ACH	Air changes per hour, h^{-1}
ACH_r	Air-changes-per-hour ratio, –
BRI	Biological Risk Index, %
C	Mass concentration, $\mu g \cdot m^{-3}$
CFD	Computational Fluid Dynamics
C_{N_i}	Particle counts per volume of size channel i, $\mu g \cdot m^{-3}$
C_{Out_i}	Outdoor mass concentration, $\mu g \cdot m^{-3}$
D_i	Mean diameter of size channel i, μm
i	Size channel (0.3, 0.5, 1, 2.5, 5, 10), –
IAQ	Indoor Air Quality
IEC	Indoor Environmental Conditions
$I/O\ Ratio$	Indoor/Outdoor ratio, –
K_i	Deposition rate of size channel i, h^{-1}
LSE	Least Squares Error, %
m_i	Mass of one particle of size channel i, μg
N	Particle counts, –
n	Number of resuspension events, –
n_{Class}	Counts for a specific conservation class, –
n_{Total}	Total number of measurements, –
PCI	Particle Conservation Index, %
PM	Particulate Matter, $\mu g \cdot m^{-3}$
P_i	Penetration factor of size channel i, –
R^2	Coefficient of determination, –
R	Reduction coefficient, –
t	Timestep, h
TGM	Tracer Gas Method, –
TPM	Total Particulate Matter, $\mu g \cdot m^{-3}$
V	Volume of the space, m^3
v_i	Deposition velocity of size channel i, $m \cdot s^{-1}$
V_s	Sample volume, m^3
x	Measurement, $\mu g \cdot m^{-3}$
$\overline{x}_{day}$	Daily running average of measurement x, $\mu g \cdot m^{-3}$
ρ	Particle density, $\mu g \cdot m^{-3}$

1. Introduction

Historic buildings classified as world heritage play a key role in nowadays society. Unique places that keep passing on values, memories, and experiences from their cultural context and collections. Many of these buildings house historic museums or libraries with very specific IEC to ensure adequate conditions for the preservation of the collections.

Considering the ten agents of deterioration proposed by Brokerhof et al. (2017), four are key parameters of a good environment for conservation: contaminants; light, temperature, and relative humidity. Contaminants, for example, can affect collections cumulatively and irreversibly, depending on the composition and sensitivity of the materials. Not only do these promote chemical reactions (acidification, corrosion, *etc.*), but can also cause physical damage to collections (abrasion, color fading, or disintegration) (Nazaroff and Cass, 1991). Surface soiling and darkening have also been observed in several studies, leading to irreversible deterioration (Anaf et al., 2013). In addition, particles can be the cause of moistening due to their hygroscopic behavior (Anaf et al., 2015), which accelerates the degradation process of the collections' materials. Therefore, the urgency to avoid any degradation of cultural objects due to poor IAQ motivates the study of particles in heritage buildings. In this context, several studies have been developing and applying different methods to monitor indoor air pollution – additional details on these studies can be found in Table S2 of the Supplementary Material (Saraiva et al., 2023).

From the review of studies on Particulate Matter (*PM*) in historic buildings using the Scopus database, a total of 79 studies were found whose titles met the following query: "particle or particulate" AND "historic OR heritage OR museum". From this list, 43 were analyzed to produce Fig. 1, which shows the categorization of different types of methodologies found.

The study of particles in historic buildings can be divided into two main areas: airborne and deposited particles. Airborne particles are usually measured with polytetrafluoroethylene (PTFE) or quartz filters installed in ventilation systems (Cao et al., 2011; Mašková et al., 2020) or recurring to particle counters (Peter et al., 2012; Roshanaei and Braaten, 1996). When the particles are collected at the filter level, the mass and chemical concentrations can be evaluated using different techniques (gravimetry (Cavicchiolia et al., 2014), X-ray emission (Gysels et al., 2002), or ion chromatography (Bartl et al., 2016), for example). When counting particles, the mass concentrations for each size channel can be estimated by knowing or assuming the composition of the particle samples (Mašková et al., 2015). There are also analytical approaches to calculate indoor mass concentrations using various mass models (Mašková et al., 2016; Mleczkowska et al., 2017), where several variables must be calculated (infiltration, penetration, and deposition). For more details, the authors recall the review study of Chen and Zhao (2011). Finally, Computational Fluid Dynamics (CFD) approaches are rarely used in this kind of study (Grau-Bové et al., 2016; Grau-Bové et al., 2019). Deposited particles can also be measured or estimated. The measurement of deposited particles requires the use of passive collectors, which accumulate dust deposited on the surfaces of the building (Anaf et al., 2015; Ozga et al., 2009). Samplers may be taken to a laboratory to have their chemical composition evaluated (López-Aparicio et al., 2011). Furthermore, other methodologies examine the loss of gloss of glass tiles to quantify the deposition in buildings (Adams et al., 2002; Ford and Adams, 1999; Smith et al., 2011). As for analytical approaches, deposition flux and velocity are usually estimated in some studies (Nazaroff et al., 1990; Chatoutsidou and Lazaridis, 2019). There are even studies where both analyses, airborne and deposited, were carried out simultaneously (Bartl et al., 2016).

Those methodologies added an important contribution to identifying the causes of indoor pollution. The main causes of indoor pollution are associated with human activities, in most cases: tourism (Lazaridis et al., 2018), cleaning (Xiu et al., 2015), and operation, followed by the building itself (collections (Barbosa et al., 2021) and furniture (Wang et al., 2015)) and its envelope (infiltration and openings (Bertolin et al., 2018; Marcelli et al., 2020)), and/or the outdoor environment (pollution (Mašková et al., 2020; Mleczkowska et al., 2017), rainfall (Injuk et al., 2002), wind (Fermo et al., 2020)).

In summary, Fig. 1 shows the common focus of the literature on monitoring mass concentrations of airborne particles in historic buildings. In contrast, particle counting is one of the least used methods for analyzing indoor air pollution. However, this approach could be particularly useful in heritage buildings where there are no centralized systems for ventilation and air conditioning, and where dust can be collected. Therefore, there is a recognized need to further explore the contribution of particle counters as a tool for the continuous monitoring of particles in historic buildings and how they can be used to assess conservation conditions. Is this type of equipment suitable for long-term and spatial analyses? There are still doubts on how monitoring should be exploited as a successful contribution to the preservation, in particular on the conservation assessment of conditions. Thus, the first objective of this study is to conduct a long-term analysis of indoor air pollution using particle counters in a heritage building. For this purpose, a monitoring campaign was conducted in a case study to evaluate the results in identifying the causes of pollution. At the same time, spatial analysis was considered in addition to temporal measurements when identifying pollution sources using particle counters, such approaches are usually resource-intensive in terms of equipment (Bulletins, 2021). This motivates the second objective of the present study: to understand the benefits of conducting spatial monitoring for conservation purposes for this particular type of equipment. Thus, the present study provides the opportunity to propose a methodology that combines long-term and spatial monitoring and how both complement each other in the assessment of conservation status. It adds a contribution to the need for pollution monitoring using particle counters to assess the

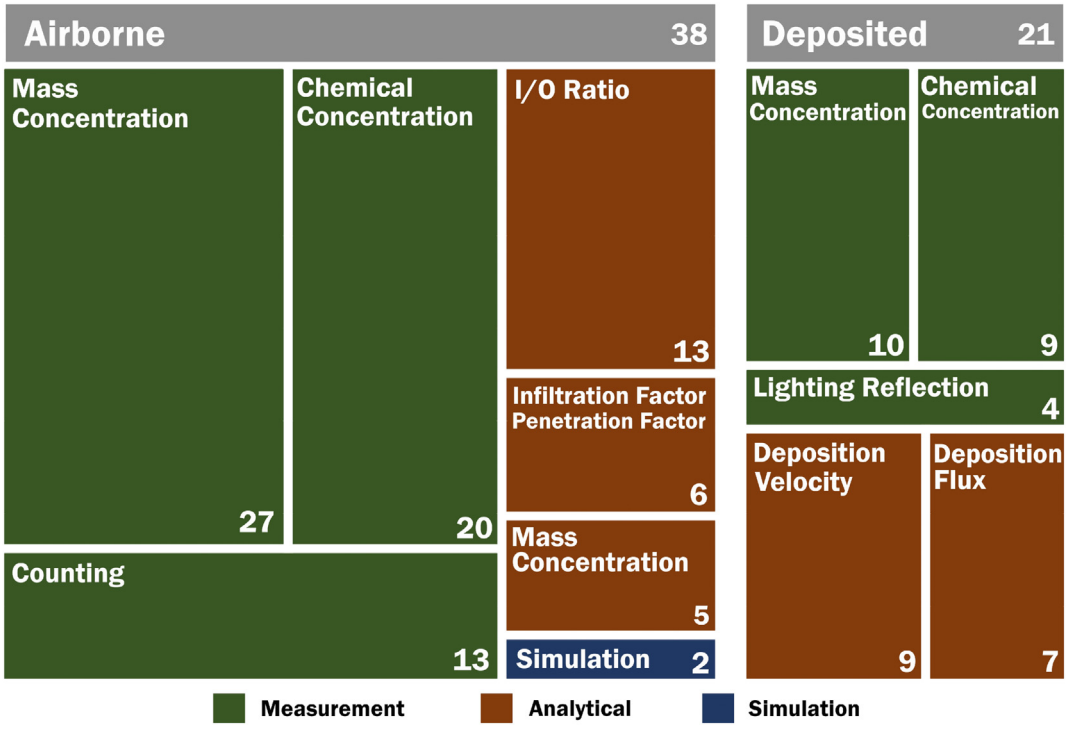

Fig. 1. Synthesized summary of the typology of studies regarding the Particulate Matter (*PM*) in heritage buildings based on Table S1 (Saraiva et al., 2023).

preservation quality and identify the main causes and sources of pollution in historic buildings. Each objective is targeted by measuring particles within a case study. The first objective involved long-term monitoring in the Joanina Library at the University of Coimbra (Portugal) and the second involved spatial monitoring of particles with multiple instruments for one month in the same library.

2. Material and methods

2.1. Case study

2.1.1. Joanina Library, University of Coimbra

As part of the World Heritage Site classified by UNESCO, the Joanina Library is the most visited monument in Coimbra, due to its historical and artistic value – over 500,000 visitors in 2017 (RTP, 2018). The construction of the building began in 1717 and was completed in 1728. It is divided into three floors, with the noblest floor, a Baroque-style space, being the focus of this study. It is richly decorated with wooden shelves painted with frescoes and gold leaf, making it one of the most unique libraries in the world – Fig. 2. The Noble Floor houses 40,000 books, mainly from the 16th and 18th, consisting of leather cases and paper, in the two-story bookshelves separated by a balcony, inaccessible to tourists.

Until the COVID-19 pandemic, tourism management was based on the intense presence of visitors with a high daily demand that allowed up to 60 visitors every 20 min between 09h00 and 19h00 (summer) and 09h00 and 17h00 (winter). Each group of tourists enters the building through the lower floor, The Prison Floor, then the visitors pass through the intermediate floor, which is referred to as Basement in this study, and finally

(a) At the ground level. (b) On the balcony floor.

Fig. 2. The Noble Floor of the Joanina Library.

reach the Noble floor, where they stay for 10 min. The tour ends with the tourists leaving the Noble Floor through the main door in direct contact with the outdoors.

Previous studies of short campaigns, two-week-long in 2017, showed high levels of indoor *PM* (Pereira et al., 2017) – 228.76 ± 239.00 $\mu g \cdot m^{-3}$, which motivated the continuous study of particle dispersion in this building.

2.2. Monitoring

The monitoring methodology was divided into two main tasks/strategies: long-term monitoring (I.), and spatial monitoring (II.). Each task was aligned with the proposed objectives of this study. The details of each task can be found in Table 1.

Task (I.) - Long-term monitoring: this task included four years of measurements using particle counters on the Nobel floor and Basement. A sensor was placed in Space 1 ($S1_F$) as shown in Fig. 3. This space is the busiest visiting area of the historic library, where tourists enter the main floor and stay the longest, and then leave through the main door. Besides tourism and door openings, during the pandemic COVID-19, the windows were usually open for ventilation purposes, especially in the summertime.

As a way to improve this long-term monitoring, a particle counter was used in several places. At the beginning of the monitoring campaign, a device was positioned on the floor from which tourists come to the Noble Floor, the Basement. It was located there until the end of October 2018, when it was moved to Space 2 ($S2_F$) until September 2019 (Fig. 3). Finally, the same device was positioned in Space 3 ($S3_F$) until the end of the study, covering periods when the building was closed to tourism due to the pandemic restrictions. The building was closed from March 18 to May 22, 2020, and from January 15 to May 31, 2021. Data were collected at each of these three locations (Basement, $S2_F$, and $S3_F$) for almost a year.

All devices were placed at the same height (1.2 m above the floor). In total, Space 1 was monitored for four years (since 1st September 2017), and the other spaces (Basement and Spaces 2 and 3) were monitored for one year long.

Task (II.) - The spatial monitoring: the number of devices was increased to expand the spatial coverage of air pollution assessment within and around the case study. As the building is located at the heights of the city hill, attached solely on the northern side, it was suspected that each façade of the building is exposed to different exterior wind and dust conditions. Therefore, outdoor monitoring was also conducted by placing the devices placed on each building's façade with openings (doors and/or windows), represented by O_N, O_S, and O_E. Those devices were installed outside in front of each façade, being placed at the windowsills of the glazing systems (O_N and O_S) and on the main door frame (O_E). Additionally, more devices were also distributed in each one of the three indoor spaces of the historic library ($S1_F$, $S3_F$, $S1_B$, $S2_B$, and $S3_B$). Vertical distribution was also evaluated by placing the devices on the balcony. A total of seven devices were used, as depicted in Fig. 3. It is noteworthy that the electric power was shut down every night. Even though all devices were equipped with a battery, monitoring could not be extended more than 2 h after the shutdown (the equipment battery autonomy).

Table 1
Summary of the two monitoring tasks carried out.

Task	Period	Equipment	Timestep
I. Long-term monitoring			
Fixed position	1st Sep 2017 1st Sep 2021	$S1_F$	10 min
Changing position[a]	3rd Nov 2017 22nd Oct 2018	Basement	
	22nd Oct 2018 06th Sep 2019	$S2_F$	
	21st Sep 2019 1st Sep 2021	$S3_F$	
II. Spatial monitoring			
	2nd Jul 2021 6th Aug 2021	Fixed positions: 5 (indoor) 3 (outdoor)	5 min

[a] One of the devices changed position several times over the monitoring period.

2.3. Workflow

The workflow of the present study followed the sequential methodology shown in Fig. 4. The measurement phase included particle counting, as the main assignment of the present work, and auxiliary tasks such as the building survey, CO_2, and outdoor monitoring.

When planning monitoring campaigns using portable optical particle counters it is important to consider memory and number of cycles, autostart, and good reliability. For the purpose of this study, devices should have an automatic turning on with a timestep of 5 and 10 min between measurements and a considerable storing memory. Considering the given requirements, Lighthouse Handheld 3016 IAQ optical particle counters were used as presented in Table 1. According to the manufacturer's manual, these devices have a counting efficiency of 50 % for particles with diameters up to 0.3 μm, and 100 % for particles with diameters > 0.45 μm complying with the ISO 21501-4 standard. Such devices operate with a sampling airflow rate of 2.83 l/m and store up to three thousand records in memory. In addition, they start automatically electrical energy is supplied. The devices were set up to take measurements every 10 min (or 5 min depending on the task), sampling for 1 min (2.83 l) and waiting 9 min (or 4 min).

To ensure the regular quality of measurements, a cleaning routine was carried out in each device whenever data were collected (every two weeks). Following the manufacturer's recommendation, a purge filter was then connected to the sample inlet for 30 min to clean each device from any residual particles. Moreover, an official brand representative calibrated all equipment in the middle of the experimental campaign (two years).

All records were analyzed and processed, having the data filtered and reordered, with time steps rounded to the nearest 5 or 10-min period depending on the task.

Apart from particles, two other monitoring activities were carried out simultaneously: indoor CO_2 concentrations and outdoor environmental conditions (temperature, relative humidity, rain, and wind – direction and speed). Indoor CO_2 was monitored as a tracer gas at the $S1_F$ location using an Onset HOBO MX1102 data logger. CO_2 measurements were used to estimate the Air Exchange per Hour (*ACH*) of each space. The meteorological parameters were measured using a Davis Instruments Vantage Pro 2 weather station, located near the case study building. A summary of the outdoor conditions during the period of study can be found in Fig. S1 (Saraiva et al., 2023). Relative humidity and precipitation were used to assess eventual correlations with indoor pollution. Hourly outdoor *PM* concentrations were collected from 2017 to 2019 from another station also in Coimbra from the QualAr project of the Portuguese Agency for the Environment (APA - Agência Portuguesa do Ambiente, 2021). A time-series graph of the evolution of the outdoor PM_{10} is presented in Fig. S2 (Saraiva et al., 2023).

2.3.1. Conversion

The conversion phase comprises the calculation of *C* and *PM* of the recorded particle counts. Given the *N* by each device, the following methodology was adopted to estimate *C*, which was adapted from Peter et al. (2012). In sum, C_i can be estimated by the following equations:

$$C_{N_i} = N_i / V_s \quad (1)$$

$$C_i = C_{N_i} / m_i \quad (2)$$

$$m_i = 1/6 \cdot \pi \cdot {D_i}^3 \cdot \rho \quad (3)$$

$$PM_i = PM_{i-1} + C_{i-1} \quad (4)$$

C_{N_i} – particle counts per unit of volume of size channel *i* [m^{-3}]; N_i – particle counts of size channel *i*; V_s – sample volume, 0.0028 [m^3]; C_i – mass

Fig. 3. Floor plans of the Joanina Library with the distribution of equipment in red markers and respective measuring directions. Task (I.): $S1_F$, $S2_F$, and $S3_F$; Task (II.): $S1_F$, $S1_B$, $S2_F$, $S3_F$, $S3_B$ O_N, O_S, and O_E.

concentration of size channel i [μg·m^{-3}]; m_i – mass of one particle of size channel i [μg]; D_i – mean diameter of size channel i [μm]; ρ – density, 2.2·1012 [μg·m^{-3}]; PM_i – particulate matter [μg·m^{-3}]; i – size channel (0.3, 0.5, 1, 2.5, 5, 10).

All instruments provide measurements for six channels (i): 0.3, 0.5, 1, 2.5, 5, and 10 μm, resulting in mean diameters of 0.4, 0.75, 1.75, 3.75, 7.5, and 10 μm, respectively. It was assumed that the density of the particles was constant, 2.2·10^{12} μg·m^{-3} based on the preliminary analysis of the measurement results where it was concluded that the courtyard was the main source of indoor PM in the case study. The outdoor pavement consists of a combination of a reactive binder with a calibrated natural gravel. So, the adopted density of particles was specified by the manufacturer's technical data sheet for this type of pavement material.

2.3.2. Estimation

To tackle the lack of measurements during the night, size-fractioned mass concentrations (C) were calculated for each day in the estimation phase. The analytical solution of the indoor mass balance model (Mašková et al., 2016) was used to predict the particle concentration during the night for each size channel – represented by Eq. (5). The mass balance model considers deposition, penetration, and emission of particles over time. During the night, it was assumed a well-mixed air environment with all doors and windows closed in each space (the building closes after 17h00/19h00 during the winter/summer).

$$C(t_j) = C_{out}(t_j)\cdot P_i\cdot ACH_r\cdot R + C(t_{j-1})\cdot(1-R)$$

$$ACH_r = \frac{ACH}{K_i + ACH} \tag{5}$$

$$R = 1 - exp\left[-(K_i + ACH)\cdot(t_j - t_{j-1})\right]$$

C_{t_j} – mass concentration for a given time t_j [μg·m^{-3}]; R – Reduction coefficient; ACH_r – air changes per hour ratio; ACH – air changes per hour for

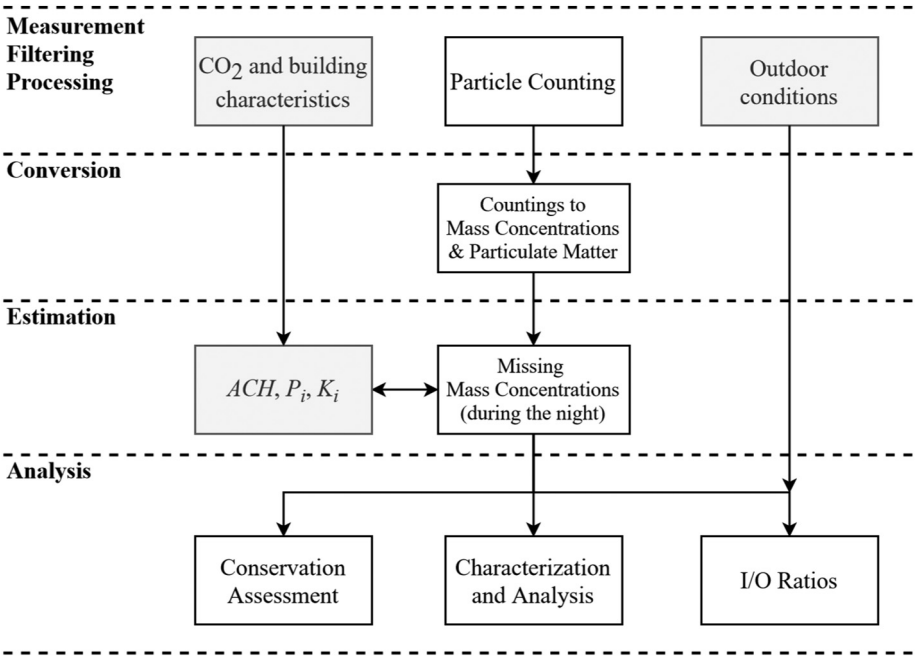

Fig. 4. Workflow of the study.

a specific day/season [h^{-1}]; P_i – Penetration factor; $C_{Out_i}(t_j)$ – outdoor mass concentration for a given time t_j [$\mu g \cdot m^{-3}$]; K_i – Deposition rate [h^{-1}]; i – size channel (0.3, 0.5, 1, 2.5, 5, 10); t_j – timestep of record j [h].

The estimation of night concentrations using Eq. (5) required a set of assumptions to simplify the approach. Firstly, the emission of new particles was neglected ($S_i = 0$) since no significant indoor sources were identified in the building. Then, it was assumed that the outdoor mass concentration C_{out_i} was constant for each night instead of varying over time and the indoor air volume was fully renovated overnight. Such assumptions were needed in order to overcome the study limitation of having only indoor monitoring: the limited resources of the study did not allow to have simultaneous monitoring of indoor and outdoor pollution. As such, C_{out_i} was considered equal to (*i*) the first record of the next day, or (*ii*) the following record of a peak first reading since a common phenomenon was noticed – the air movement induced by the cleaning personnel in the morning was leading to very high first readings. This value could not be used as C_{out_i} for the estimation during the previous night. Instead, whenever this phenomenon happened, the second record of the next day was used to avoid mispredictions.

The remaining inputs, air changes per hour (*ACH*), penetration factor (P_i), and deposition rate (K_i), were estimated. In the study of the airtightness of each space, the Noble Floor and Basement, CO_2 measurements were used to estimate the *ACH* through the tracer gas method (*TGM*) and its decay during the night (unoccupied period). This method is fully described in ISO 12569:2017 (ISO, 2017). *ACH*s were computed for each day and stored whenever a Coefficient of Determination (R^2) of 0.80 was achieved. Whenever it was not possible to estimate *ACH* using the CO_2 tracer method on a specific day of Space 1 and Basement, average seasonal *ACH*s were used instead.

The deposition rate (K_i) was estimated considering the approach proposed by Zhao and Wu (2007), by estimating K_i for each space (1, 2 and 3), considering its volume, and the areas and roughness of surfaces. A sensitivity analysis was carried out by changing roughness values from very smooth to very rough. Such sensitivity analysis contributes to the understanding of the impact of roughness on the calculation of K_i and P_i in the several spaces. However, for the conservation analysis described in Subsection 2.3.3, a very rough environment was considered for all spaces on the Noble floor (Space 1, 2 and 3), and a rough one for the Basement. This assumes that all surfaces are extremely detailed with contours that increase the overall roughness of the library's inner surfaces.

The deposition rate (K_i) is directly proportional to the deposition velocity (v_i) and a constant ratio between the area of all surfaces (A) and the space volume (V) (Lai and Nazaroff, 2000). Deposition velocities depend on the particle size, following the values pointed out by Zhao and Wu (2007), and density, being then corrected according to a review study (Grau-Bové and Strlič, 2013).

The penetration factor (P_i) could be calculated if outdoor concentrations (C_{out_i}) were known (Chen and Zhao, 2011). Since C_{out_i} was assumed, an alternative approach needed to be followed. An iterative process using Eq. (5) was done to estimate the indoor mass concentrations [$C(t)$] and, at the same time, compute the P_i. For this purpose, all data between 17h00 and the last record's time was used to validate the best combination of the two variables that were progressively changed in Eq. (5). The variables were the P_i and the initial point of the temporal evolution ($C_{(t=0)}$). For each cycle, the P_i ranged from 0 to 1, with increments of 0.05, and the initial point $C_{(t=0)}$ was the u-th minimum (for particles of 0.3 and 0.5 μm of diameter) or maximum (for the remaining particles) of that period for further estimation. The initial point changed at least 10 times ($u = 10$), as the first, second, and so on, until the tenth, minimum/maximum value between 17h00 and the final day record. This totalized 200 combinations for every cycle. The best combination was chosen based on the lowest Least Squared Error (*LSE*) and the highest Coefficient of Determination (R^2). Then, it was used to estimate concentrations during the night giving a continuous trend to the on-site measurements required for the conservation assessment.

2.3.3. Analysis

The continuous data set for the measured locations were used to analyze and evaluate the results regarding the quality of conservation of collections during the monitoring period. For the assessment of the conservation conditions, the present study proposes a new methodology to classify *PM* measurements in historic buildings from the point of view of preservation considering the survey of the most used conservation norms and thresholds, as detailed in the Supplementary Material (Saraiva et al., 2023). Due to differences between norms' maximum *PM* thresholds, it was recognized the need to develop a standardized method for classifying pollution conditions to fill this gap. Moreover, norms refer only to static conditions at a given time, *t*, neglecting the effects of a continuously poor environment on preservation. Only Tétreault (2003) included in the analysis the temporal assessment of measurements and their consistency. This way, it is defined a

Table 2
Thresholds for the conservation methodology.

Degradation risk		Class A	Class B	Class C	Class D
PM [$\mu g \cdot m^{-3}$]		Low	Moderate	High	Extremely high
$PM_{2.5}$ thresholds	Measurement (x)	< 1	10	50	> 50
	Daily running avg ($\bar{x}_{day}$)	< 0.5	5	10	> 10
PM_{10} thresholds	Measurement (x)	< 10	30	75	> 75
	Daily running avg ($\bar{x}_{day}$)	< 5	10	30	> 30

new classification system with two input parameters, the *PM* measurement, x, and the daily moving average of *PM*, $\bar{x}_{day}$. Less strict values of the standards were used as a reference for each conservation class of x, while more restrictive thresholds were used for the classification of $\bar{x}_{day}$. This indicator $\bar{x}_{day}$ is an average value calculated from the previous 24 h for a given time, t, to assess the quality of indoor air pollution over time. Maximum values for each parameter are presented in Table 2, while the logical sequence to classify the conditions in a given moment is presented in Fig. 5.

The authors named Performance Conservation Index (*PCI*) to the presented methodology, which includes an analysis of peak events, whenever the $\bar{x}_{day}$ complied with the class thresholds but *PM* concentrations, x, in a specific time, t, was double the x of the next timestep, $t + 1$, a count n is made to register a peak event. In this case, the conservation class should not be affected if it is for a very short period. This is a similar approach to the existing one for the IAQ assessment for health reasons (Portaria n.o 353-A/2013, 2013). In other words, the maximum values can be punctually

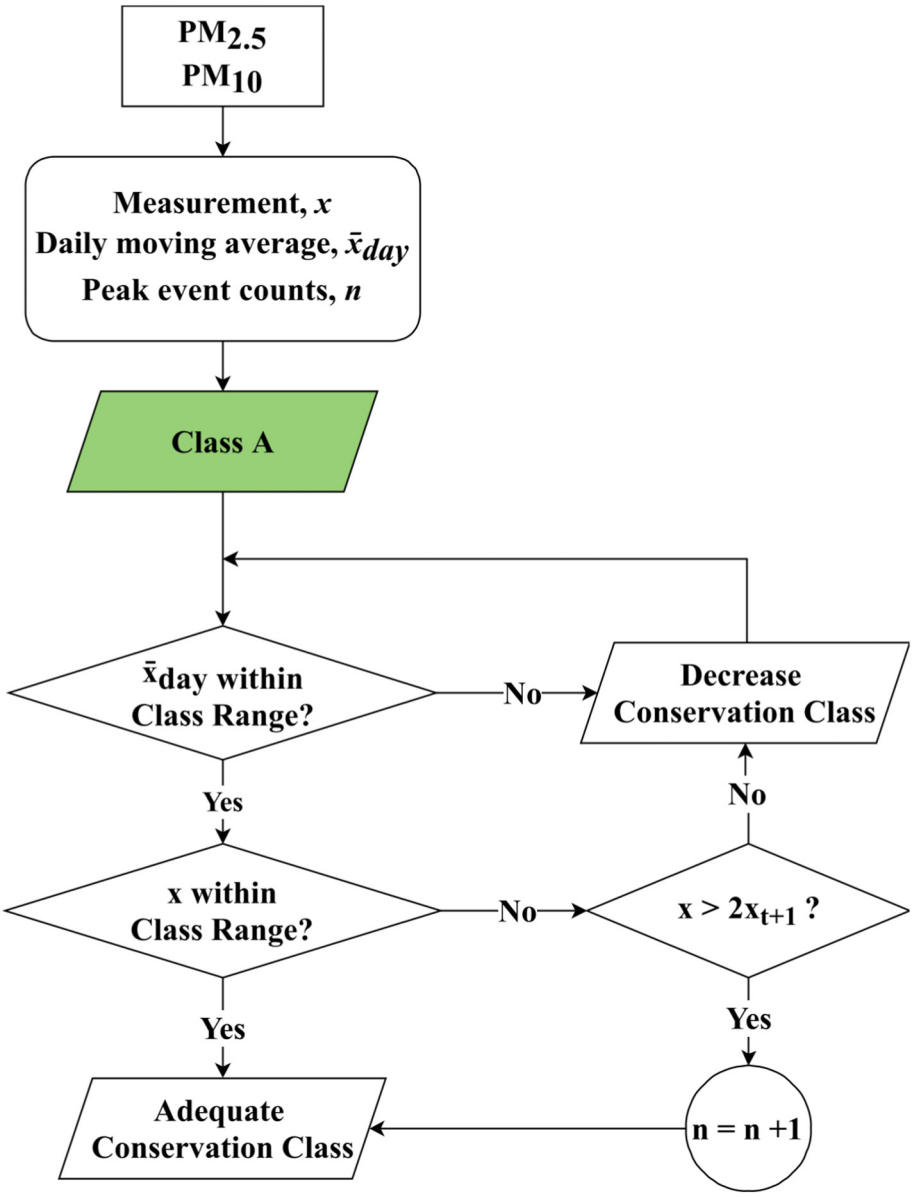

Fig. 5. *PCI* classification methodology.

exceeded if the daily average remains below the referenced limit. This methodology emphasizes the significance of the indoor pollution stability over a day rather than a punctual measurement during the day. Nonetheless, it does not mean peaks should be neglected as they are also important to identify patterns and relations to activity events. This categorization is not intended to be compulsory, but it may be used to help conservators and curators interpret measurements in a more standardized way as an auxiliary tool to recommended values in conservation norms.

The Performance Conservation Index (*PCI*) was estimated for each of the conservation classes, which represent the risk of degradation and range from A (low) to D (extremely high). This corresponds to the compliance of the measurements according to the respective maximum values

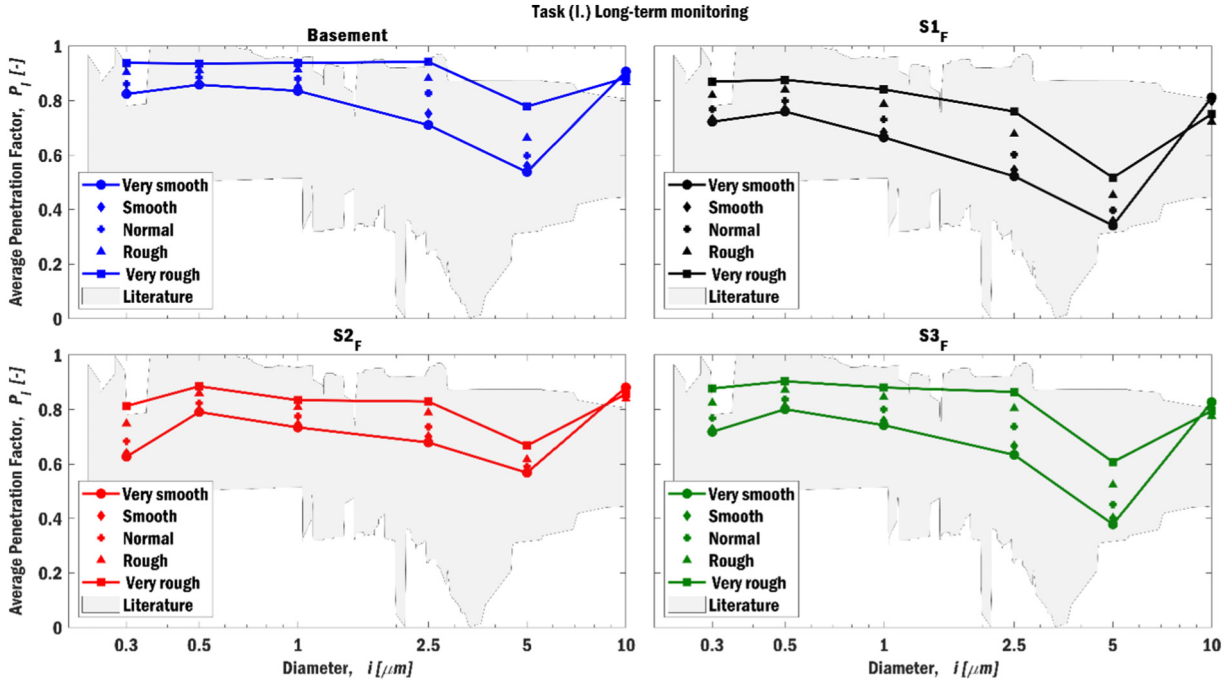

(a)

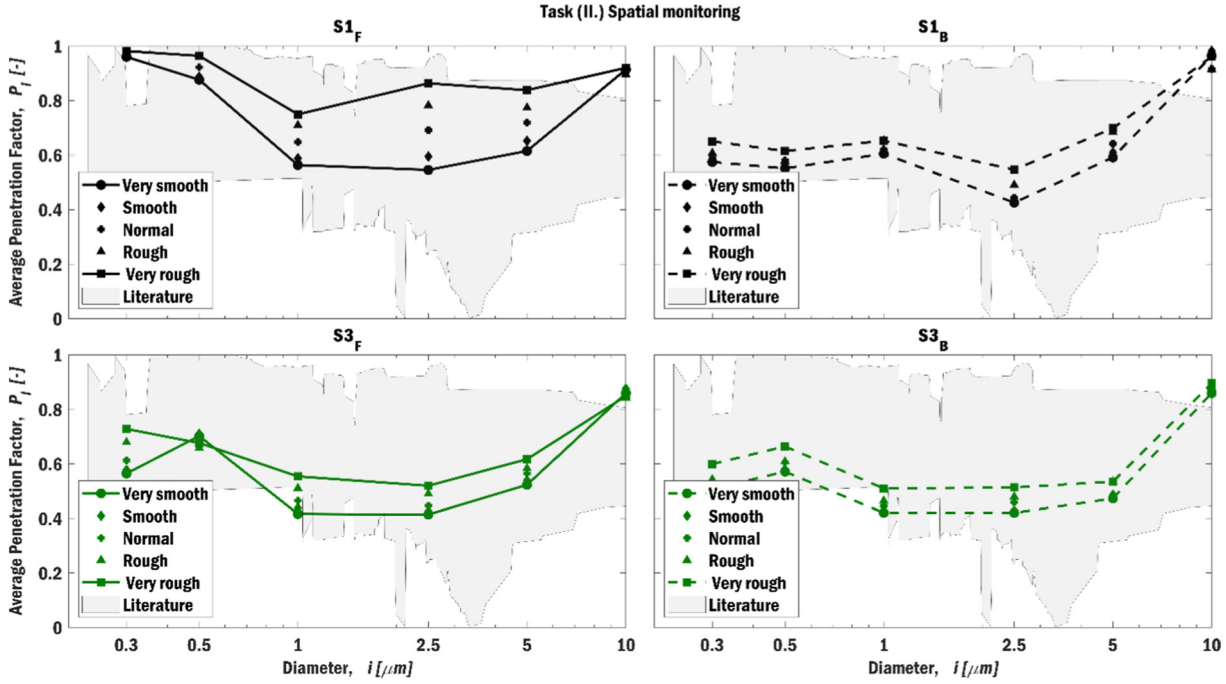

(b)

Fig. 6. Average P_i in (a) Task (I.), long-term analyses, and (b) Task (II.), spatial analysis, for each size channel in all spaces.

recommended by the standards in Table 2. In other words, *PCIs* represent the percentage of time that measurements are within a specific conservation class as expressed in Eq. (6).

$$PCI = n_{Class}/n_{Total} \cdot 100 \quad (6)$$

PCI – Performance Conservation Index [%]; n_{Class} – counts for a specific conservation class; n_{Total} – total number of measurements in the monitoring campaign.

The last part of this study includes the calculation of the *I/O Ratios* using both concentrations (indoor and outdoor), expressing the relationship between the indoor and outdoor environment. Though there are recognized limitations, mainly to quick variations of this estimator since it is influenced by several circumstances (Chen and Zhao, 2011), it was assumed a steady-state condition of the indoor environment for each timestep (Mašková et al., 2020).

3. Results

3.1. (I.) Long-term monitoring

The building airtightness was characterized by seasonal averages of *ACH* of 0.32, 0.38, 0.42, and 0.34 h^{-1} for the Winter, Spring, Summer, and Autumn periods, respectively. Such values resulted from the estimation of *ACH* in 540 days through the night decay of CO_2 that was carried out along with the particle counting – please consider Fig. S3 (Saraiva et al., 2023).

Deposition rates (K_i) were estimated for Space 1, 2, and 3 and the Basement considering different roughness according to the sensitivity analysis described in Subsection 2.3.2. It was assumed that Space 1 and 3 had similar deposition contexts, since they are identical spaces, while Space 2 varies in terms of area. K_i varied from 0.002 to 0.234, 0.004 to 0.201, 0.009 to 0.203, 0.05 to 0.301, 0.199 to 0.541, and 0.840 to 1.540 for the respective size channel (0.3, 0.5, 1, 2.5, 5 and 10) depending on the adopted roughness. A graphical representation of K_i is shown in Fig. S4 (Saraiva et al., 2023). Maximum K_i were found for the roughest, while the minimum were registered for smoother surfaces.

The estimation of the P_i along with the sensitivity analysis in Fig. 6 presents the results regarding the average P_i for each size channel in both tasks.

The estimated values during the night of a very rough environment for the Noble floor rooms and rough for the Basement were used in the analysis of mass concentrations and the respective conservation assessment. The distribution of particles (measured and estimated) was analyzed in terms of size within the building as presented in Fig. 7.

In general terms, particles with an aerodynamic diameter of 5 μm were the most common followed by the 2.5 μm-diameter size ones. The biggest disparity in mass concentrations occurs for particles with diameters of 1 μm that fit within the $PM_{2.5}$ size channel. Another considerable increase in mass concentrations is noticed between size channels of 0.5 and 1 μm. This is in concordance with what was reported in the literature (Grau-Bové and Strlič, 2013), meaning that, in heritage buildings, it is relevant to analyze PM_1, especially when this type of building is visited as smaller particles are more dangerous to human health.

The complementary monitoring of three different locations (Basement, $S2_F$, and $S3_F$) within the Joanina Library was carried out in different periods to compare the mass concentrations with the reference zone in Space 1 ($S1_F$). Therefore, the statistical analysis shows that in the contiguous spaces of the Noble Floor ($S1_F$, $S2_F$, and $S3_F$), the mass concentrations (*C*) were not the same for all channels. The most polluted room was Space 2 ($S2_F$), followed by Space 1 ($S1_F$), then Space 3 ($S3_F$, and $S3_F$), and the Basement. If the analysis is focused on each size channel, results differ depending on the aerodynamic diameter of particles from space to space. $S2_F$ was more polluted with particles with diameters > 1 μm, while the Basement had more particles with smaller diameters (< 1 μm).

For conservation purposes, size-fractioned mass concentrations were converted to *PM* for two size channels, $PM_{2.5}$ and PM_{10}, along with the respective *PCIs*. Fig. 8 shows in detail the distribution of each measurement using the *PCI* methodology, which was developed in this work. The compliance with other conservation norms is presented in Table S4 (Saraiva et al., 2023).

In general terms, the compliance with *PCI* was rarely adequate, regardless of the particle size and space location since Class A had very low *PCIs*, being Class C ($PM_{2.5}$) and Class D (PM_{10}) the most common. This highlights the poor quality of the indoor environment for conservation purposes within the case study. While fine particles ($PM_{2.5}$) are less frequent, thus presenting higher compliance with better conservation classes, coarse particles are much more common reflecting on the poorest conservation classes. Punctual resuspension events (*n*) are highlighted in red in Fig. 8,

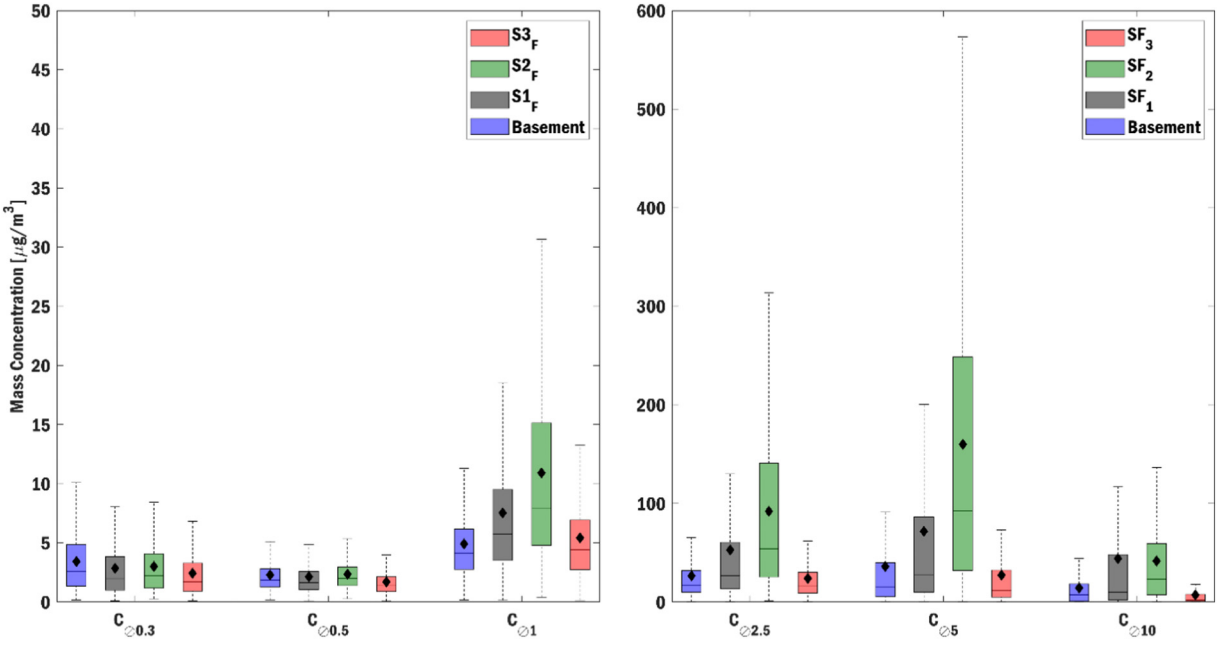

Fig. 7. Statistical analysis for particle measurements per size-channel in the Joanina Library: Basement (23,388 measured and 13,637 estimated), $S1_F$ (100,110 measured and 70,282 estimated), $S2_F$ (18,224 measured and 17,474 estimated), and $S3_F$ (48,077 measured and 29,460 estimated).

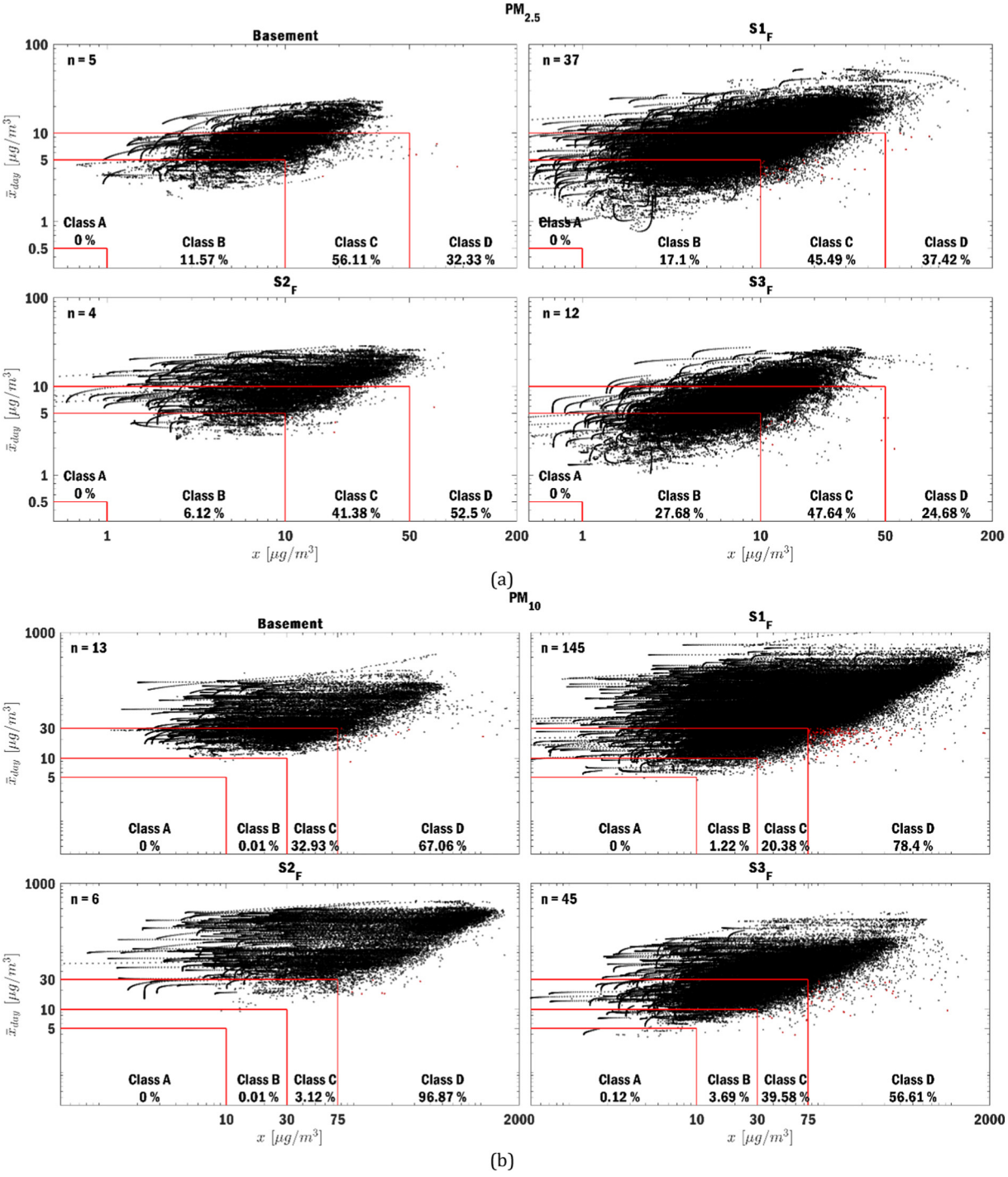

Fig. 8. *PCI* matrices for (a) $PM_{2.5}$, and (b) PM_{10} in the four locations. The points corresponding to punctual resuspension events (*n*) are highlighted in red.

occurring only a few times compared to the number of measured points. Notwithstanding, the new conservation assessment method *PCI* provides a steadier classification of indoor pollution considering a temporal analysis without jeopardizing resuspension events. Therefore, this method can be used as an alternative classification to other norms' when analyzing the conservation of collections from a preventive preservation point of view.

Daily average data from the nearby weather station was used to estimate *I/O Ratio* of the daily averages of PM_{10} in Space 1 ($S1_F$). The calculated *I/O Ratio* showed that the indoor concentrations were always higher than outdoors, as it was always > 1 (*I/O Ratio* > 1) during the total monitoring period. Within this period, 33.3 % of the time the *I/O Ratio* of the daily averages ranged between 1 and 3, 50 % between values of 3 and 10, and 16.7 % higher than 10 (> 10). Such results indicate some accumulation and/or resuspension were occurring inside the building since *PM* concentrations were always higher indoors than outdoors. However, it was not possible to estimate *I/O Ratio* for the several size channels. This was discussed in the literature as a relevant aspect of indoor pollution characterization since *I/O Ratio* strongly depends on particle size (Chatoutsidou et al., 2015). Adding to this, the nearby weather station is not located exactly in the same place as the case study. So, combining the need of measuring different size channels

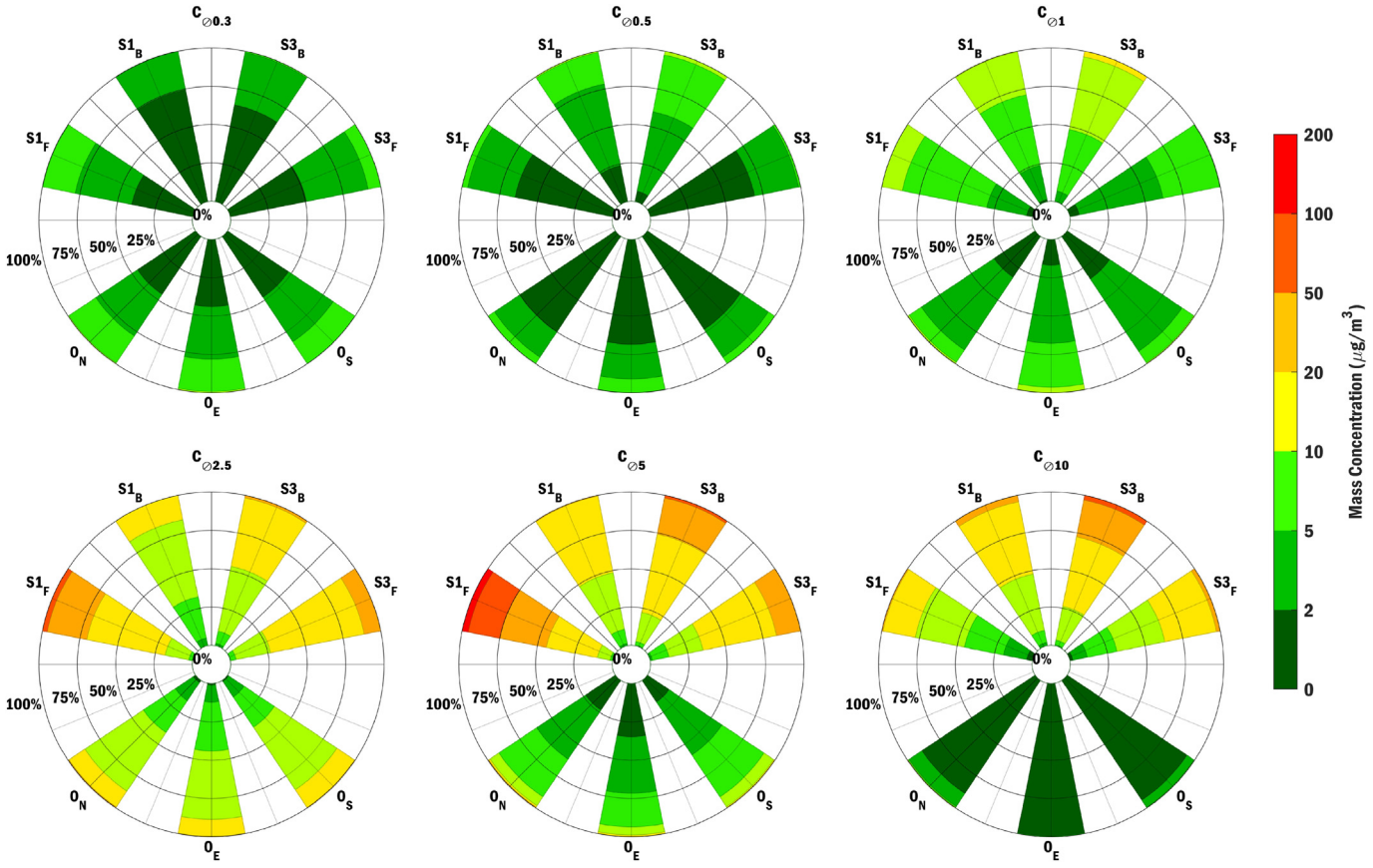

Fig. 9. Size-fractioned mass concentrations of the spatial monitoring.

with the on-site outdoor monitoring campaign, the second part of the present study targeted this opportunity. In Task (II.) an outdoor monitoring campaign in front of each façade of the building was performed for one month, which allowed estimating the *I/O Ratio* for each size channel with on-site outdoor measurements.

3.2. (II.) Spatial monitoring

The dedicated monitoring of the spatial distribution of particles gave a simultaneous perspective of the vertical and horizontal gradients along the library. To correctly compare concentrations in terms of spatial

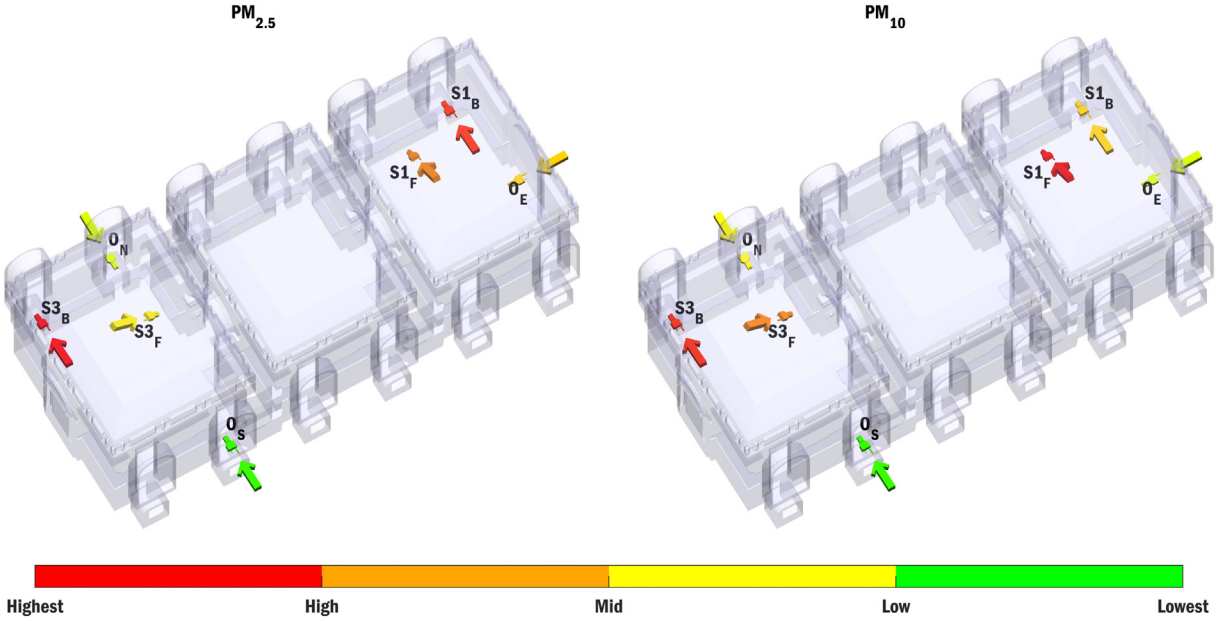

Fig. 10. 3D spatial representation of the equipment with the respective ranking of pollution for $PM_{2.5}$ and PM_{10} channels.

distribution, all measurements were synchronized by timestep to ensure the same quantity of data in every location. The overall results are presented in the form of cumulative distributions of the size-fractioned mass concentrations (C_i) in each space for each one of the monitored size channels. The set of graphs in Fig. 9 presents the results of size-fractioned mass concentrations (C_i) during this campaign.

In terms of size-fractioned mass concentrations (C_i), particles with 0.3 and 0.5 μm of diameter presented low values of pollution, not exceeding 10 $\mu g \cdot m^{-3}$. For 1-μm diameter particles, mass concentrations reached 20 $\mu g \cdot m^{-3}$, while channels 2.5 and 10 did not exceed 100 $\mu g \cdot m^{-3}$. Larger concentrations were mostly found at the 5-μm channel, reaching up to 240 $\mu g \cdot m^{-3}$.

In terms of the horizontal gradient at the floor level, Space 1 ($S1_F$) is more polluted than Space 3 ($S3_F$), except for the 10-μm size channel. While at the balcony level, Space 3 ($S3_B$) is the most polluted as shown in Fig. 9. These conclusions are generally observed regardless of the size of the particles. In terms of vertical gradient, the size of particles interferes with the distribution of particles since the same pattern is identified in both Spaces 1 and 3. The floor level ($S1_F$ and $S3_F$) is more polluted than the balcony ($S1_B$ and $S3_B$) for size channels 0.3 and 2.5, while the opposite

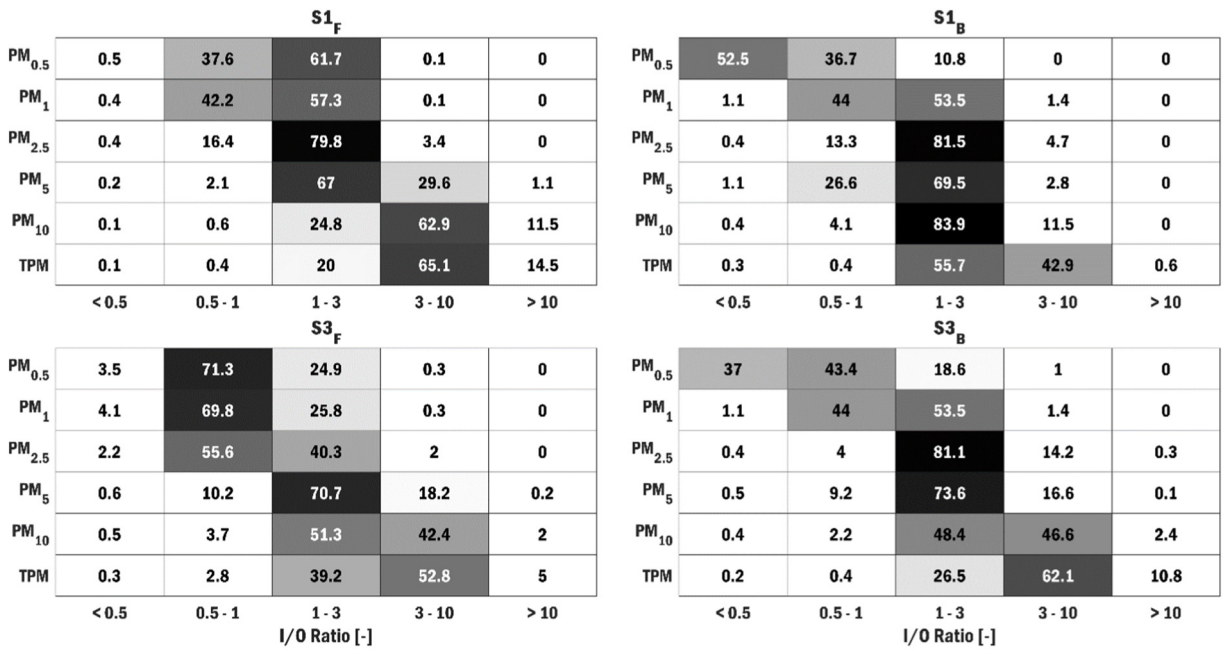

(a)

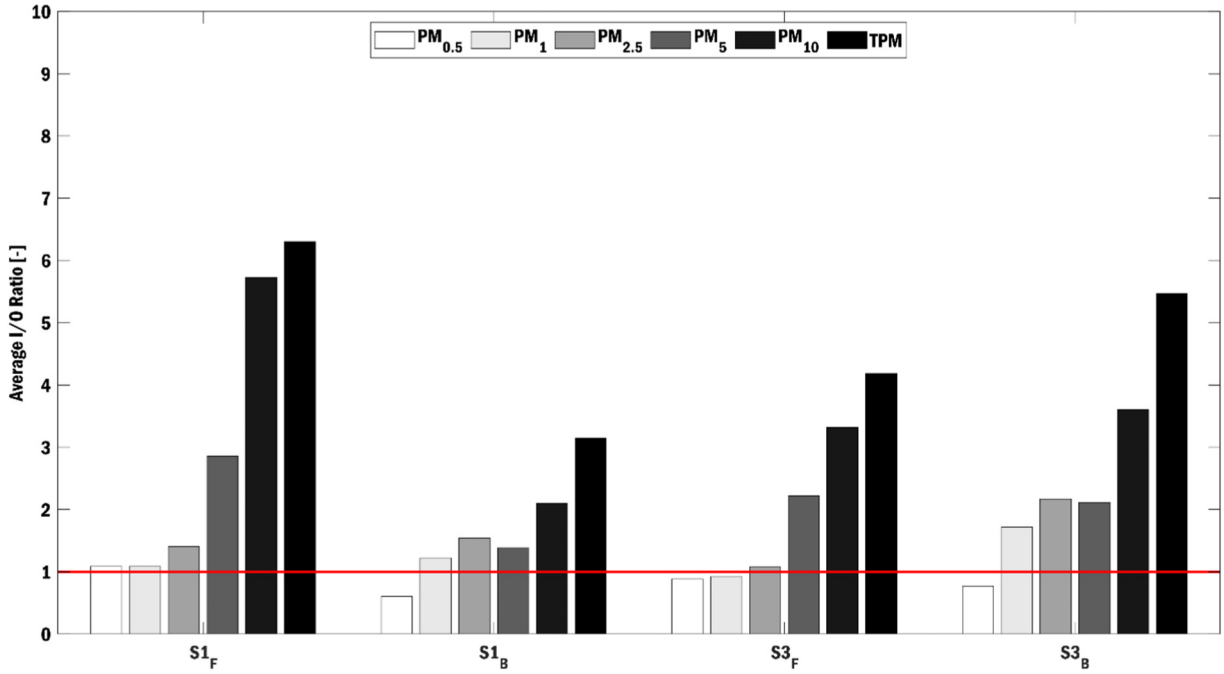

(b)

Fig. 11. Results of the Task (II.): (a) Distribution of percentages among ranges of I/O ratio values; and (b) averages of I/O ratios for each location and size channel.

occurs for particles with diameters of 0.5, 1, and 10. The only difference between the vertical gradient between both spaces is in the 5-μm size channel where in Space 1 ($S1_F$) it is more polluted than in the balcony, and in Space 3, the balcony is more polluted ($S3_B$). For these differences, no correlation was found between the vertical gradient and the size of particles. Still, it can be noted that $S1_F$ has a major source of pollution that has an evident impact on this size channel (5-μm), which is precisely the most polluted size-fractioned channel of all locations in the long-term campaign — the causes of pollution are discussed in the following section.

Regarding outdoor concentrations, the three façades presented similar results except for the 1-μm size channel — check Fig. 9. It was expected that particle concentrations on the East side of the building (O_E) would be higher than in the other orientations since this façade is facing the open-air sanded courtyard without any obstructions. However, size-fractioned mass concentrations of OE are only greater for small particles: 0.3, 0.5, and, with major differences, in 1-μm channels. This could indicate that infiltrations through the eastern façade and its openings could have a greater impact on indoor pollution on the 1-μm channel rather than on others. Nonetheless, when comparing indoor and outdoor concentrations, it is observed (Fig. 9) that indoor pollution is usually higher than outdoors, except for the 0.3-μm size channel. On the contrary, particles sized equal to 5 and 10 μm on the three outdoor devices registered concentrations considerably low, probably due to the fact that these bigger particles are heavier and deposited, being less common in suspension in the outdoor environment. Converting mass concentrations into *PM*, it was possible to plot the average results of $PM_{2.5}$ and PM_{10} size channels according to their location within the library as shown in Fig. 10.

PM concentrations were then used to calculate *I/O Ratio*. The discriminated percentages of the *I/O Ratio* within certain ranges for each location are presented in Fig. 11. Regardless of the device location, the most common bin of *I/O Ratio* varied between 1 and 3. This points out that the indoor environment is commonly more polluted than the outdoor one. It is also noticeable that *I/O Ratio* tends to increase with the increase in particle size, which indicates that there are larger accumulations of bigger particles indoors. $PM_{0.5}$ and PM_1 were the only channels that had *I/O Ratio* below 1 most of the time depending on the location, which is aligned with what was presented in the last paragraph.

Averages are also presented in the last graph of Fig. 11. On average, *I/O Ratio* ranged between 0.5 and 4.5, though reached up to 6 in $S1_F$ for PM_{10} and Total Particulate Matter (*TPM*) channels. The increase of *I/O Ratio* with the increase of *PM* size channel is highlighted by the ladder shape presented in Fig. 11. Lower ratios were estimated for $PM_{0.5}$ and PM_1, while higher ratios were for PM_{10} and *TPM*.

4. Discussion

The validation of the indoor mass balance model, using records after the closing time of the building, converged to the Penetration factor (P_i) with the best performance for each time step *t* for each roughness considered. The threshold of 0.70 to R^2 as a good agreement between predictions and measurements of particulate matter (Saraiva et al., 2021). With this reference value in mind, the compliance between the measured and estimated values shows a satisfactory performance of the indoor air mass model, which resulted in R^2 values of 0.73, 0.70, 0.70, 0.71, 0.70, and 0.69 for all size channels of *PM* concentrations in the Basement, $S1_F$, $S2_F$, and $S3_F$, respectively. Nevertheless, the approach implemented to estimate concentrations tends to underpredict concentrations as can be seen in Figs. S7 to S10 (Saraiva et al., 2023).

The sensitivity analysis points out that P_i are usually higher on rough models than on smoother ones regardless of the space and task, with the exception of size channel 10 μm where the pattern is inverted. For both tasks, differences between P_i for different values of roughness are almost constant suggesting a linear correlation where P_i increase with the increase of roughness. Moreover, such differences have the same dispersion for Task (I.), but in the second task, $S1_F$ presents a different increase of P_i with the increase of roughness for size channel 2.5 and 5 μm, which is related to the bigger concentrations monitored in this space.

The only possible comparison of P_i results between both tasks is done for $S1_F$ and $S3_F$ locations. The longer campaign gives a more representative idea of the penetration of particles to spaces since it has a more complete

Table 3
Comparison of *PM* measurements (averages ± standard deviation) of Task (I.) with other case studies.

Literature	Averages [μg·m^{-3}]	Basement	$S1_F$	$S2_F$	$S3_F$
PM_1					
Mašková et al. (2020)	1.4–9.4	5.7 ± 4.1	4.9 ± 3.7	5.3 ± 3.7	4.1 ± 3.3
Mašková et al. (2015)	0.2–12				
Krupińska et al. (2013)	5–12				
Deering et al. (2019)	8–42				
$PM_{2.5}$					
Anaf et al. (2013)	8–17	10.6 ± 5.7	12.5 ± 8.8	16.2 ± 9.8	9.5 ± 5.9
Cao et al. (2011)	108.4–242.3				
Cavicchiolia et al. (2014)	3.5–5.8				
Marcelli et al. (2020)	9–9.8				
Krupińska et al. (2013)	12–32				
Deering et al. (2019)	10–50				
Lazaridis et al. (2015)	28–52				
PM_{10}					
Anaf et al. (2013)	12–31	72.9 ± 87.7	136.7 ± 180.7	268.2 ± 261.8	60.6 ± 67.2
Mašková et al. (2020)	2–10.3				
Cavicchiolia et al. (2014)	8.6–11.2				
Mašková et al. (2015)	0.2–25				
Mašková et al. (2016)	4–30				
Lazaridis et al. (2018)	19–44				
Marcelli et al. (2020)	11–15				
Krupińska et al. (2013)	10–18				
Deering et al. (2019)	21–82				
Lazaridis et al. (2015)	32–62				
TPM					
Cao et al. (2011)	172.4–312.5	87.1 ± 107.4	180.8 ± 262.5	309.8 ± 307.7	65.7 ± 79.3
Hu et al. (2009)	220.6				

dataset, even though, dynamic outdoor concentrations (C_{out_i}) were used in the estimation of penetration factors (P_i) for the spatial task. Generally, P_i results were different when comparing the same locations for the different tasks. For $S1_F$, the second task presented greater P_i values, while $S3_F$ presented much smaller values in the second task.

In Task (I.) the Basement presented the biggest P_i values, while the remaining spaces presented a similar pattern. The Basement has a smaller area where particles can deposit comparing to the Noble floor, which is highly decorated with details and edges. Therefore, the Basement has lower K_i and, in return, increased P_i values to compensate estimation algorithm of the indoor air balance model. $S2_F$ was the space with lower differences when changing roughness values. The remaining location presented similar results for P_i.

In Task (II.), it is possible to evaluate differences within the same space but at different heights. Differences are more noticeable in Space 1 where at the floor level ($S1_F$), P_i are bigger than on the balcony level ($S1_B$). On Space 3 results are identical. It is also perceived that the balcony results have similar patterns.

Regardless of the task, P_i of particles with diameters of 10 μm are the only values that are outside of the literature range. In fact, In the literature, P_i tends to diminish as the diameter of particles increases, so it was expectable that results for this size range would follow the downtrend of P_i (decreasing with the increase of the size of particles). This is related to the faster deposition of larger particles, which are mostly settled in this specific size channel, which forces bigger P_i during the iterative process. However, the results do not show this downtrend, P_i increases for particles with diameters of 10 μm in both tasks. For the long-term part of the study, it may be justified by the assumption of having the outdoor concentrations constant and equal to the first value in each day indoor for the long-term task. If this outdoor value registered was lower (most of the particles are/were settled) P_i needed to increase in the indoor mass balance model to converge to the measured indoor measurement for the estimation phase. For the spatial task, instead of using a constant value during the night in Eq. (5), dynamic outdoor concentrations (C_{out_i}) were used in the estimation of penetration factors (P_i). However, very few particles with that diameter were counted during the campaign, indicating that those particles were settled and, such as in the first task, the best performance value for P_i to compensate for measured indoor concentrations. Mašková et al. (2020) had already reported difficulties related to the P_i of bigger particles.

In terms of *PM*, measurements led to the confirmation that the indoor environment was: i) polluted through the characterization of mass concentrations; and, consequently, ii) more polluted indoors than the outdoor through the estimation of *I/O Ratio* using *PM*; reflected in iii) the poor IAQ for conservation of cultural patrimony. In this way, *PM* concentrations measured at Joanina Library in Task (I.) can be compared to the results found in other case studies — please consider Table 3.

From Table 3, for size channels PM_1 and $PM_{2.5}$, results were within those found in the literature. However, for PM_{10} Joanina Library has larger measured averages compared to other case studies. Total Particulate Matter (*TPM*) is only presented in Table 3 to show the only case study where PM measurements were within the same range as those found in Joanina Library. The Emperor Qin's Terracotta Museum (Cao et al., 2011; Hu et al., 2009) presents a similar range of values, which also has a sanded pavement like the Joanina Library courtyard. It is important to highlight that Task (II.) was carried out during a period of less touristic presence due to the COVID-19 pandemic. Thus, the reduction of visitors affected *PM* measurements, diminishing the obtained values to similar ranges in other case studies. Even so, the different context and operation of Joanina Library justify the larger measurement of particles compared to the other case studies. The unique combination of factors related to the building itself led to the high measurement of indoor particles.

Source: courtyard — A punctual *PM* measuring in other buildings, that surround the Joanina Library and share the same courtyard, showed that indoor pollution is related to its sanded pavement: the same size pattern was identified in all the buildings that surround the courtyard as evidenced in Fig. S5 (Saraiva et al., 2023). When tourists walk over the sanded courtyard, the thin gravel is smashed into dust, and, then, brought indoors (Fig. S6 (Saraiva et al., 2023)). In literature, problems related to the outdoor pavement have rarely been addressed in touristic sights (Hu et al., 2009), being this specific case study a relevant contribution to raising awareness of its negative impact on this type of building.

Transportation: tourists – It was observed that particles, which were adhered to the footwear and clothing of visitors as they walked through the sanded courtyard, were then brought inside. Since tourists were the

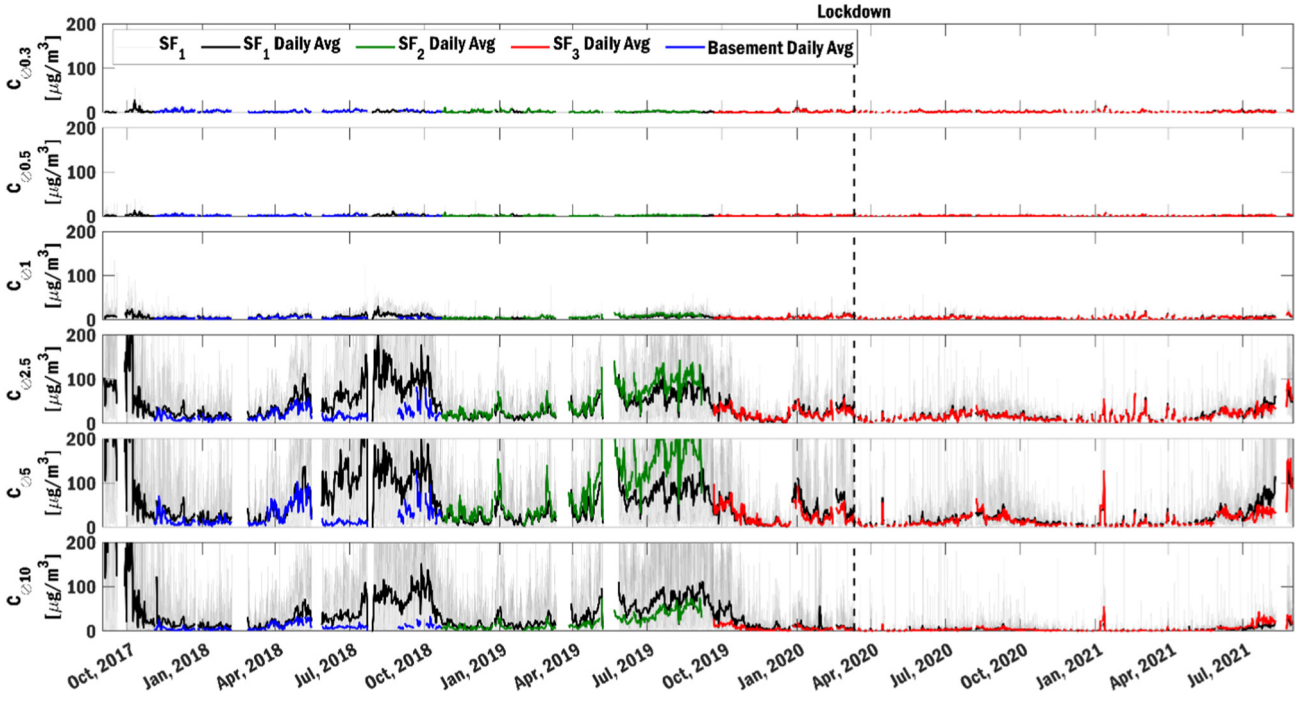

Fig. 12. Long-term analysis of the particle concentration by size channel in the Joanina Library.

main transportation means between the outdoor and the indoor, the opportunity left by the lockdown due to the COVID-19 pandemic allowed to evaluate this concern. In this way, Fig. 12 evidences that indoor pollution reduced abruptly with the lockdown, clarifying that the increase of particles is related to tourism. The correlation coefficients between measurements and daily tourism rates were 0.02, 0.17, 0.60, 0.72, 0.71, and 0.74 for each size channel (0.3, 0.5, 1, 2.5, 5, and 10 μm, respectively). This indicates a strong correlation for particles with diameters > 1 μm. Similarly, other studies have been reporting tourism as a major driver of indoor pollution, promoting resuspension (Chatoutsidou et al., 2015) and bringing dust adhered to their clothes (Bertolin et al., 2018). In this library, the strong correlation between tourists and dust ends up reflecting the improvement of the conservation conditions during the lockdown. Where $PM_{2.5}$ and PM_{10} were reduced by 64.6 % and 28.5 %, respectively.

Deposition: carpet – Particles transported indoors were accumulated on the building since.

I/O Ratio indicates a more polluted environment indoors. Another agent of pollution that the literature points out is textiles (Marcelli et al., 2020). Carpets can act as a deposit of particles that when walked by tourists enhanced resuspension (Injuk et al., 2002). The analysis of time-series plotting (Fig. 12) showed that when the carpet was removed from the Basement floor on May 28th 2018, when concentrations dropped considerably. This proved that a considerable amount of dust was being deposited on the carpet, and then, resuspended. Thus, a week-long trial without the long-red carpet on the Noble Floor allowed to confirm the positive impact of not having carpets on intensely visited buildings as highlighted in Fig. 13.

Resuspension: carpet and tourists — Visitors were responsible for transporting particles indoors and the carpet acted as a deposit. However, the combined effect of having tourists walking on carpets enhanced resuspension (Serfozo et al., 2014; Rosati et al., 2008). This is the sole reason why mass concentrations present similar trends every day. *PM* peaks occurred before lunchtime, and then, in the afternoon, before the closing time due to tourism activity. Whenever a new visit is entering the noble floor, new particles are being deposited and the already deposited ones are resuspended. This ends up increasing dust particles (between 2.5 and 10 μm). Then, this duo "carpet-tourists" is the major contributor to indoor pollution. Therefore, the use of textile carpets on the floor is discouraged (Wang et al., 2015), and literature recommends using vinyl carpets instead (Camuffo, 1996) on heritage buildings that are highly visited.

Another resuspension type of event was noticed since occasionally the first readings on a day were very high. This was related to the cleaning personnel movement, which has also been discussed in other studies (cleaning procedure activities boost resuspension, such as opening and moving books (Deering et al., 2019), or cleaning the buildings (Xiu et al., 2015)).

Other patterns can be investigated, *e.g.*, a seasonal pattern is noticed over the years (Fig. 12), especially for bigger particles, associated with the outdoor conditions. The diminishing of particle concentrations whenever it rains has been reported in other studies (Prajapati, 2003; Sánchez de la Campa et al., 2011), as particles settle when watered. Fig. 13 shows the explicit effect of rain on *PM* reduction. Drought has also been related to the increase in particle suspension (Fermo et al., 2020). Regarding the relation between indoor pollution and the wind speed measured at the weather station, no noticeable patterns were found probably due to the distance of the station to the case study.

Some other studies registered higher concentrations during the winter (northern hemisphere), justifying the seasonal variability due to an increase in outdoor pollution (Cao et al., 2011; Fermo et al., 2020) – but that was not the case. Likewise, the presence of fungi or mold could be contributing to the increase of particles, especially for particles with diameters up to 10 μm (PM_{10}). For this purpose, the authors followed the methodology presented in another study (Schito et al., 2018), where the risk of mold growth was assessed using the same case study. Therefore, the estimation of the Biological Risk Index (*BRI*) was done for the long-term analysis in $S1_F$ and $S3_F$ where hygrothermal data loggers were placed. However, results indicate a low biological risk of mold growing and spore germination, as for $S1_F$, $S2_F$, and $S3_F$, percentages were 1.39 %, 0.03 %, and 5.90 %, respectively. Nevertheless, a microbiological sampling should be done to evaluate and confirm the presence of fungi and/or mold.

Fig. 14 presents the evolution of *PM* concentrations in the outdoor and indoor environments allowing an evaluation of the outdoor results and their impact on the indoor environment.

Fig. 14 illustrates the greater impact of the outdoor environment on the indoor pollution of $PM_{2.5}$ than on PM_{10} since the daily evolution of indoor concentrations follows the outdoor ones of the former size channel. Marcelli et al. (2020) have already reported that indoor particles usually

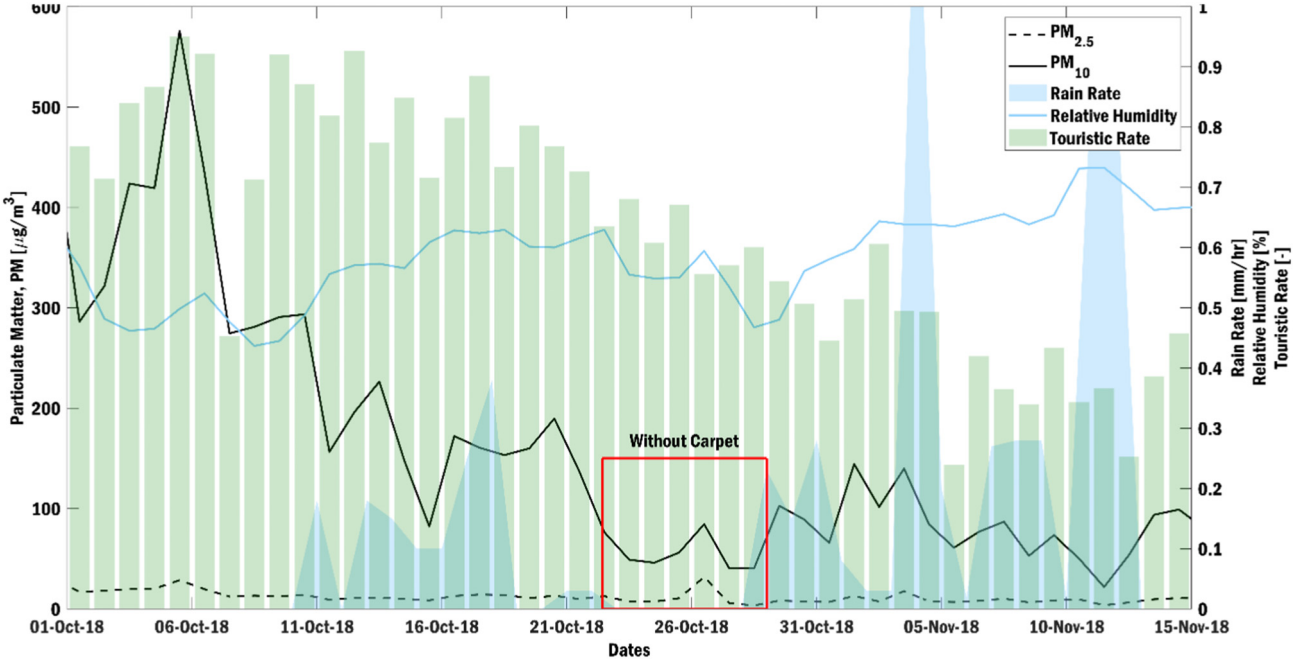

Fig. 13. Average values of daily *PM* concentrations, rain rates, relative humidity, and touristic rates in periods with and without carpet (red box). The inverse relation between precipitation (blue area) and pollution is also notorious.

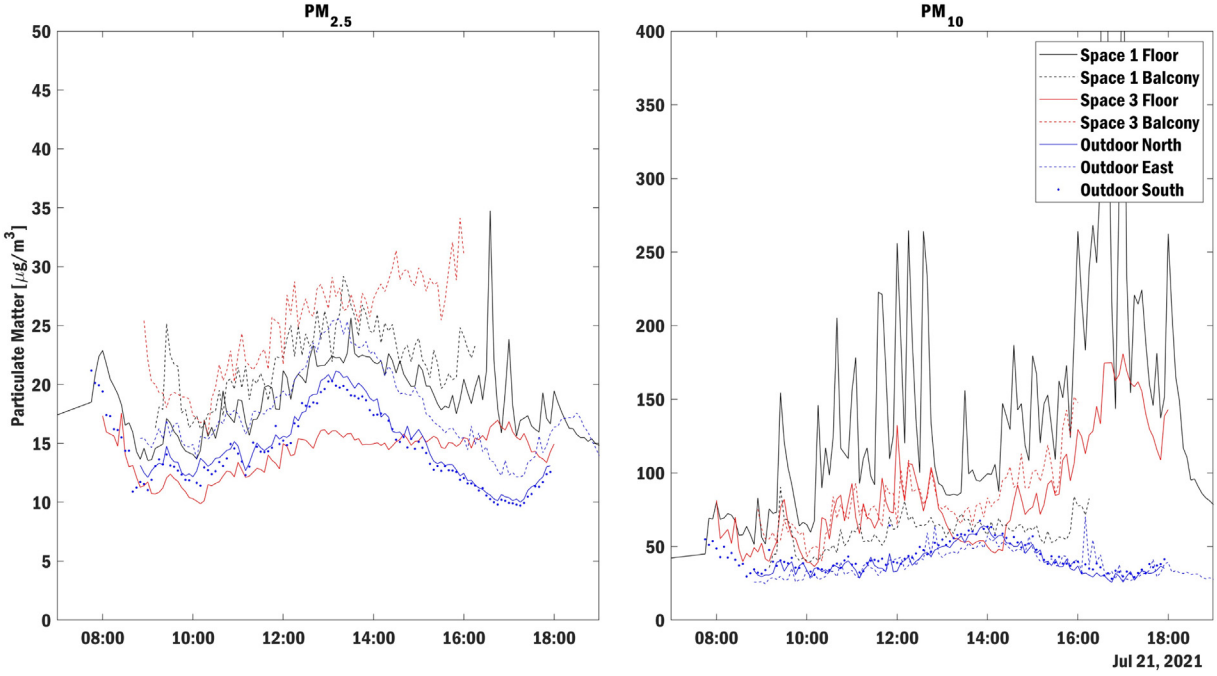

Fig. 14. Daily graph of the spatial monitoring.

follow the outdoor trends but for both $PM_{2.5}$ and PM_{10}. But herein, on the contrary, PM_{10} trends show that an increase of particles is more related to resuspension due to tourism as it was discussed previously as a driving source of pollution. This affects the *I/O Ratio* calculated on both tasks, where the analysis is done for each channel. Task (II.) allowed a closer analysis of the *I/O Ratio* since outdoor pollution was being measured exactly on the building location, it was done for the 6 size channels and with smaller timesteps than those used on Task (I.).

For channel PM_{10} in $S1_F$, results were similar between both tasks (33.3 % and 24.8 % for *I/O Ratio* between 1 and 3, 50.0 % and 62.9 % between 3 and 10, and 16.7 % and 11.5 for values > 10, for Task (I.) and (II.), respectively). Comparatively, the *I/O Ratio* for PM_{10} in four case studies in a similar study (Mašková et al., 2020) did not exceed 0.07, 0.19, 0.18, and 0.33 – these values are very different from those registered in the present study. Indeed, the results obtained during the second campaign, point out the higher differences between the indoor and outdoor on particles with diameters > 1 μm ($PM_{2.5}$). From one point of view, those *I/O Ratio* are usually bigger as there is a lot of transportation and deposition of particles within the case study. But from the other, some extreme peaks of *I/O Ratio* are related to temporary and punctual occasions of resuspension during the day – as observed in Fig. 14. This has already been discussed as a drawback of *I/O Ratio* analysis when quick variations of this parameter were influenced by punctual events (Chen and Zhao, 2011), which do not characterize indoor pollution in global terms.

I/O Ratio were calculated using measurements of O_E as it was the most potential pollution source. But, from the evaluation of the indoor monitoring and the outdoor measurement in each façade, it was verified that there was no need for more than one outdoor device. One device is sufficient to effectively characterize outdoor concentrations and estimate *I/O Ratio*, as the results were similar for the three monitored façades.

Finally, it is critical to reflect on the importance of spatial monitoring for the characterization of particle distribution using portable optical counters. Dust collection at filters is suitable to evaluate dust composition. However, there are many buildings without centralized systems to ventilate and collect dust. Thus, portable optical particle counters are useful alternatives to characterize the indoor environment for a long-term or spatial assessment of the conservation conditions as it was demonstrated in the present work. Continuous monitoring allows the allowed to identify the relation of events with the fluctuation of particles. Therefore, the characterization of the indoor pollution presented for Joanina Library using optical particle counters gave sufficient insight for an effective long-term and spatial assessment of the indoor environment, especially for conservation purposes. This idea is reinforced for heritage buildings that have several restrictions (resources, visual impact, *etc.*) as such devices are relatively small, produce less noise, and can be easily moved. Even so, some limitations can be acknowledged as the forced shutdown of energy during nighttime (counters were not running), which limited the analysis of indoor pollution during that period. Even though, this limitation was overcome by predicting the night decay concentrations, estimated using the indoor mass balance model. This model is grounded on CO_2 monitoring to use the *TGM* allowing the estimation of Air Changes per Hour (*ACH*), then, the calculation of Deposition rates (K_i), and the iterative process to estimate Penetration factors (P_i) with lower errors, R^2 and *LSE*. Such concentrations were required to implement the proposed classification of indoor pollution from a conservation perspective. This approach can be easily replicated in other case studies for the conservation assessment.

5. Conclusion

One of the greatest challenges for historic buildings that are intensively visited by tourists is the maintenance of environmental conditions and their compatibility with heritage conservation.

In the context of preventive conservation, particles and dust are among the most common threats to conservation leading to careful attention and evaluation. Commonly, monitoring and simulation approaches are the mainly used methodologies. Of all the variety of methods, particle counting is one of the least used. Therefore, the present research focuses on investigating how portable optical counters can be used for the long-term and spatial monitoring of particles in historic buildings.

To achieve this goal, two monitoring campaigns were divided into different tasks: (I.) four-year data collection with two instruments; (II.) spatial distribution of particles with seven instruments in the Joanina Library of the University of Coimbra.

These measurements were used to estimate mass concentrations, particulate matter (*PM*), *I/O Ratio*, and to assess the preservation quality. A new approach to classify *PM* was developed and applied as an alternative to the prevailing preservation standards. In this way, the use of such devices

proved to be useful for pollution sources and typical pattern identification, when compared to other studies following different approaches.

The results supported the characterization of particle suspension within the case study, particularly the particles coming from the courtyard, their transportation (tourists), deposition indoors (carpet), and the reason for their resuspension (carpet and tourists). Measurements indicated high particle suspension, particularly for particles > 1 μm throughout the long-term monitoring, reflecting poor compliance with the best conservation classes. Consequently, the optical counter data indicated a polluted indoor environment, most of which conformed to Class C and D thresholds given the novel classification used in this work.

Regarding the spatial distribution, airborne particles and their suspension depend on the size channel evaluated. In terms of vertical distribution, the balcony level was always less contaminated than the floor level for the 0.3, 2.5, and 5 μm size channels, and more contaminated for the 0.5, 1, and 10 μm channels. The horizontal distribution depends on the level at which the particles were measured.

Considering the constraints that apply to some heritage buildings (visibility, noise, and operation) and the characterization of indoor pollution using optical particle counters, such equipment can be a useful alternative to other approaches for long-term and spatial purposes. Therefore, the proposed methodology adapts the use of these devices so that they can be used in other case studies.

CRediT authorship contribution statement

Nuno Baía Saraiva: Conceptualization; Data curation; Formal analysis; Investigation; Methodology; Validation; Visualization; Roles/Writing – original draft; Writing – review & editing.

Luísa Dias Pereira: Conceptualization; Data curation; Investigation; Methodology; Writing – review & editing.

Adélio Rodrigues Gaspar: Conceptualization; Formal analysis; Funding acquisition; Investigation; Methodology; Project administration; Resources; Supervision; Writing – review & editing.

José Joaquim Costa: Conceptualization; Formal analysis; Funding acquisition; Investigation; Methodology; Project administration; Resources; Supervision; Writing – review & editing.

Data availability

Data will be made available on request.

Declaration of competing interest

The authors declare the following financial interests/personal relationships which may be considered as potential competing interests:

Nuno Baia Saraiva reports financial support was provided by Fundação para a Ciência e a Tecnologia (FCT). Luisa Dias Pereira reports financial support was provided by Fundacao para a Ciencia e a Tecnologia (FCT) & MCTES (PIDDAC).

Acknowledgments

The research presented has been developed under the Energy for Sustainability Initiative of the University of Coimbra (UC).

Funding

The work of the first author was partially funded by the Rectory of the University of Coimbra (UC) under the framework of the project "BJUC-AHT Monitorização e análise do ambiente interior na Biblioteca Joanina da Universidade de Coimbra", and the doctoral Grant "SFRH/BD/151356/2021" financed by the Portuguese Foundation for Science and Technology (FCT), and with funds from the "European Social Fund" (FSE) and "Programa Por Centro" part of the Government Funds, under MIT Portugal Program. The work of the second author was carried out in the framework of Project UIDP/50022/2020 - LAETA - Laboratório Associado de Energia, Transportes e Aeronáutica, with the financial support of FCT/MCTES through national funds (PIDDAC).

Appendix A. Supplementary data

Supplementary data to this article can be found online at https://doi.org/10.1016/j.scitotenv.2022.160747.

References

Adams, S.J., Kibrya, R., Brimblecombe, P., 2002. A particle accumulation study during the reconstruction of The Great Court, British Museum. J. Cult. Herit. 3 (4), 283–287.

Anaf, W., Horemans, B., Madeira, T.I., Carvalho, M.L., De Wael, K., Van Grieken, R., 2013. Effects of a constructional intervention on airborne and deposited particulate matter in the Portuguese National Tile Museum, Lisbon. Environ. Sci. Pollut. Res. 20 (3), 1849–1857.

Anaf, W., Bencs, L., Van Grieken, R., Janssens, K., De Wael, K., 2015. Indoor particulate matter in four belgian heritage sites: case studies on the deposition of dark-colored and hygroscopic particles. Sci. Total Environ. 506–507 (2015), 361–368.

APA - Agência Portuguesa do Ambiente, 2021. QualAr Project - Dataset of PM concentrations for Coimbra.Available: https://qualar.apambiente.pt/downloads [Accessed: 02-Nov-2021].

Barbosa, K., Ferreira, T., Moreira, P., Vieira, E., 2021. Monitoring pollutant gases in museum microclimates: a relevant preventive conservation strategy. Conserv. Património, May,no. 28, 22–34.

Bartl, B., Mašková, L., Paulusová, H., Smolík, J., Bartlová, L., Vodička, P., 2016. The effect of dust particles on cellulose degradation. Stud. Conserv. 61 (4), 203–208.

Bertolin, C., Strojecki, M., Kozłowski, R., 2018. Particle penetration, emission and deposition in the diocesan Museum in Udine, Italy to assess soiling of Giambattista Tiepolo's wall paintings. Stud. Conserv. 63 (sup1), 326–328.

Brokerhof, A., Ankersmit, B., Ligterink, Frank, 2017. Risk management for collections. Rijksdienst voor het Cultureel Erfgoed. Cultural Heritage Agency of the Netherlands, Amersfoort.

Bulletins, C.C.I.T., 2021. Control of Pollutants in Museums and Archives – Technical Bulletin. 37, pp. 1–58.

Camuffo, D., 1996. Controlling the microclimate and particulate matter inside the historic anatomy theatre, Padua. Museum Manag. Curatorsh. 15 (3), 285–298.

Cao, J.J., et al., 2011. Chemical composition of indoor and outdoor atmospheric particles at emperor Qin's Terra-cotta museum, Xi'an, China. Aerosol Air Qual. Res. 11 (1), 70–79.

Cavicchiolia, A., Pardini Morrone, E., Fornaro, A., 2014. Particulate matter in the indoor environment of museums in the megacity of São Paulo. Quim Nova 37 (9), 1427–1435.

Chatoutsidou, S.E., Lazaridis, M., 2019. Assessment of the impact of particulate dry deposition on soiling of indoor cultural heritage objects found in churches and museums/libraries. J. Cult. Herit. 39, 221–228.

Chatoutsidou, S.E., Mašková, L., Ondráčková, L., Ondráček, J., Lazaridis, M., Smolík, J., 2015. Modeling of the aerosol infiltration characteristics in a cultural heritage building: the baroque library hall in Prague. Build. Environ. 89, 253–263.

Chen, C., Zhao, B., 2011. Review of relationship between indoor and outdoor particles: I/O ratio, infiltration factor and penetration factor. Atmos. Environ. 45 (2), 275–288.

Deering, K., et al., 2019. Monitoring of arsenic, mercury and organic pesticides in particulate matter, ambient air and settled dust in natural history collections taking the example of the Museum für Naturkunde, Berlin. Environ. Monit. Assess. 191 (6), pp.

Fermo, P., Comite, V., Ciantelli, C., Sardella, A., Bonazza, A., 2020. A multi-analytical approach to study the chemical composition of total suspended particulate matter (TSP) to assess the impact on urban monumental heritage in Florence. Sci. Total Environ. 740, 140055.

Ford, D., Adams, S., 1999. Deposition rates of particulate matter in the internal environment of two London museums. Atmos. Environ. 33 (29), 4901–4907.

Grau-Bové, J., Strlič, M., 2013. Fine particulate matter in indoor cultural heritage: a literature review. Herit. Sci. 1 (1), 1–17.

Grau-Bové, J., Mazzei, L., Malkii-Ephstein, L., Thickett, D., Strlič, M., 2016. Simulation of particulate matter ingress, dispersion and deposition in a historical building. J. Cult. Herit. 18, 199–208.

Grau-Bové, J., Mazzei, L., Thickett, D., Strlič, M., 2019. New perspectives on the study of particulate matter deposition within historic interiors. Stud. Conserv. 64 (4), 193–202.

Gysels, K., Deutsch, F., Van Grieken, R., 2002. Characterisation of particulate matter in the Royal Museum of fine arts, Antwerp, Belgium. Atmos. Environ. 36 (25), 4103–4113.

Hu, T., et al., 2009. Characterization of winter airborne particles at emperor Qin's Terra-cotta museum, China. Sci. Total Environ. 407 (20), 5319–5327.

Injuk, J., Osán, J., Van Grieken, R., Tsuji, K., 2002. Airborne particles in the Miyagi museum of art in Sendai, Japan, studied by electron probe X-ray microanalysis and energy dispersive X-ray fluorescence analysis. Anal. Sci. 18 (5), 561–566.

ISO, 2017. ISO 12569:2017 - Thermal Performance of Buildings and Materials — Determination of Specific Airflow Rate in Buildings — Tracer Gas Dilution Method.

Krupińska, B., Van Grieken, R., De Wael, K., 2013. Air quality monitoring in a museum for preventive conservation: results of a three-year study in the Plantin-Moretus Museum in Antwerp, Belgium. Microchem. J. 110 (2013), 350–360.

Lai, A.C.K., Nazaroff, W.W., 2000. Modeling indoor particle deposition from turbulent flow onto smooth surfaces. J. Aerosol Sci. 31 (4), 463–476.

Lazaridis, M., Katsivela, E., Kopanakis, I., Raisi, L., Panagiaris, G., 2015. Indoor/outdoor particulate matter concentrations and microbial load in cultural heritage collections. Herit. Sci. 3 (1), 1–13.

Lazaridis, M., Katsivela, E., Kopanakis, I., Raisi, L., Mihalopoulos, N., Panagiaris, G., 2018. Characterization of airborne particulate matter and microbes inside cultural heritage collections. J. Cult. Herit. 30, 136–146.

López-Aparicio, S., et al., 2011. Relationship of indoor and outdoor air pollutants in a naturally ventilated historical building envelope. Build. Environ. 46 (7), 1460–1468.

Marcelli, A., Sebastianelli, M., Conte, A., Lucci, F., Della Ventura, G., 2020. Micro-climatic investigation and particulate detection in indoor environments: the case of the historical museum of Bersaglieri in Rome. Rend. Lincei 31 (3), 807–817.

Mašková, L., Smolík, J., Vodička, P., 2015. Characterisation of particulate matter in different types of archives. Atmos. Environ. 107, 217–224.

Mašková, L., Smolík, J., Travnickova, T., Havlica, J., Ondráčková, L., Ondráček, J., 2016. Contribution of visitors to the indoor PM in the national library in Prague, Czech Republic. Aerosol Air Qual. Res. 16 (7), 1713–1721.

Mašková, L., Smolík, J., Ondráček, J., Ondráčková, L., Travnickova, T., Havlica, J., 2020. Air quality in archives housed in historic buildings: assessment of concentration of indoor particles of outdoor origin. Build. Environ. 180 (June), 1–10.

Mleczkowska, A., Strojecki, M., Bratasz, Ł., Kozłowski, R., 2017. The effect of ventilation on soiling by particles of outdoor and indoor origin in historical churches. Build. Simul. 10 (3), 383–393.

Nazaroff, W.W., Cass, G.R., 1991. Protecting museum collections from soiling due to the deposition of airborne particles. Atmos. Environ. 25 (5–6), 841–852.

Nazaroff, W.W., Ligocki, M.P., Ma, T., Cass, G.R., 1990. Particle deposition in museums: comparison of modeling and measurement results. Aerosol Sci. Technol. 13 (3), 332–348.

Ozga, I., Ghedini, N., Bonazza, A., Morselli, L., Sabbioni, C., 2009. The importance of atmospheric particle monitoring in the protection of cultural heritage. WIT Trans. Ecol. Environ. 123, 259–269.

Pereira, L.D., Gaspar, A.R., Costa, J.J., 2017. Assessment of the indoor environmental conditions of a baroque library in Portugal. Energy Procedia 133, 257–267.

Peter, G., Simon, X., Denis, B., 2012. Workplace aerosol mass concentration measurement using optical particle counters. J. Environ. Monit. 420–428.

Portaria n.o 353-A/2013, 2013. Ordinance no 353-A/2013 (in Portuguese: Regulamento de Desempenho Energético dos Edifícios de Comércio e Serviços (RECS) - Requisitos de Ventilação e Qualidade do Ar Interior).

Prajapati, C.L., 2003. Accumulation of solid particles on documents, a threat for preservation of documentary heritage. Restaurator 24 (1), 46–54.

Rosati, J.A., Thornburg, J., Rodes, C., 2008. Resuspension of particulate matter from carpet due to human activity. Aerosol Sci. Technol. 42 (6), 472–482.

Roshanaei, H., Braaten, D.A., 1996. Indoor sources of airborne particulate matter in a museum and its impact on works of art. J. Aerosol Sci. 27 (SUPPL.1), S443–S444.

RTP, 2018. Mais de 500 mil pessoas visitaram a Universidade de Coimbra em 2017. Available: https://www.rtp.pt/noticias/cultura/mais-de-500-mil-pessoasvisitaram-a-universidade-de-coimbra-em-2017_n1049977.

Sánchez de la Campa, A.M., de la Rosa, J.D., Fernández-Caliani, J.C., González-Castanedo, Y., 2011. Impact of abandoned mine waste on atmospheric respirable particulate matter in the historic mining district of Rio Tinto (Iberian Pyrite Belt). Environ. Res. 111 (8), 1018–1023.

Saraiva, N.B., Rodrigues, E., Gaspar, A.R., Costa, J.J., 2021. Daylighting simulation of a heritage building by comparing matrix methods and solar models. Sol. Energy 224 (January), 685–696.

Saraiva, N.B., Pereira, L.Dias, Gaspar, A.R., Costa, J.J., 2023. Supplementary Material Measurement of Indoor Pollution in Heritage Buildings Using Particle Counters: Long-term and Spatial Analyses.

Schito, E., Dias Pereira, L., Testi, D., Gameiro da Silva, M., 2018. A procedure for identifying chemical and biological risks for books in historic libraries based on microclimate analysis. J. Cult. Herit. 37, 155–165.

Serfozo, N., Chatoutsidou, S.E., Lazaridis, M., 2014. The effect of particle resuspension during walking activity to PM10 mass and number concentrations in an indoor microenvironment. Build. Environ. 82, 180–189.

Smith, A., Goodhue, R., Dublin, T.C., Bioletti, S., Dublin, T.C., 2011. Monitoring deposited dust in the old library, Trinity College Dublin. Int. Preserv. News 53, 19–23.

Tétreault, J., 2003. Airborne pollutants in museums, galleries, and archives: risk assessment, control strategies, and preservation management. Can. Conserv. Inst. (ISBN: 0662340590).

Wang, L., Xiu, G., Chen, Y., Xu, F., Wu, L., Zhang, D., 2015. Characterizing particulate pollutants in an enclosed museum in shanghai, China. Aerosol Air Qual. Res. 15 (1), 319–328.

Xiu, G., et al., 2015. Characterization of particulate matter, ions and OC/EC in a museum in Shanghai, China. Aerosol Air Qual. Res. 15 (4), 1240–1250.

Zhao, B., Wu, J., 2007. Particle deposition in indoor environments: analysis of influencing factors. J. Hazard. Mater. 147 (1–2), 439–448.